3.2. GFP expression following plasmid DNA transfection

To investigate the transgene expression and distribution, the transfected epidermis was harvested at different time points. Horizontal and vertical sections of the epidermis were viewed under a confocal laser microscope to investigate the three-dimensional, dynamic distribution of positively transfected cells. The horizontal sections revealed that a fraction of keratinocytes were transfected and expressed GFP. The fluorescent areas increased from days 2 to 7 after transfection and appeared to merge with each other by days 5–7 (Fig. 2A–C). The vertical sections showed that most of the fluorescence-positive cells migrated from the basal layer to the upper layer of the LSE between days 2 and 7 after transfection (Fig. 2D–F), while, on day 5, other cells still lagged behind (Fig. 2E), and a few persisted in the basal layer on days 5 and 7 (Fig. 2F).

3.3. Multiple GFP plasmid DNA transfections increased transgene expression in LSE

To increase the number of positively transfected cells, re-transfection was carried out. The results showed that the number of positively transfected cells increased with increasing frequency of transfection (single, double, or triple transfection), as revealed by analyzing horizontal and vertical sections of the epidermis of the transfected LSEs. Between 20 and 30% of the epidermal cells were GFP-positive (Fig. 3A–F). As seen in the vertical sections, GFP-positive cells were located mainly in the upper layer of the epidermis after single transfection and in the middle and upper layers after double transfection. Following triple transfection, GFP expression was distributed not only in the stratum corneum and suprabasal layer but also in the basal layer of the epidermis. With histogram of Zeiss LSM Image Examiner, we measured the unit fluorescence intensity on horizontal sections of three samples transfected 1, 2 or 3 times, respectively. The total intensity for each sample was counted, and the mean values of three samples were calculated. The relative fluorescence intensity of 2-time and 3-time transduction was 1.3 ($p < 0.05$) or 1.8 ($p < 0.05$) compared to 1-time transduction, respectively.

3.4. Transgene expression in transfected LSE grafts in vivo

To investigate the transgene expression in vivo, the LSEs were transplanted onto full-thickness wounds on the backs of nude mice, and samples were harvested on days 3, 5, 7, and 14 after transplantation. H&E staining of sectioned LSE grafts showed that, from day 3 up to day 14, the grafts survived well and the epidermis was well differentiated and stratified without any signs of toxicity (Fig. 4A–D). The frozen sections of the samples showed that the fluorescence-positive cells kept moving upward and were almost all restricted in stratum corneum at day 14, rarely seen at day 21 (data not shown), probably lost during skin scaling. On day 3, the GFP-positive cells stayed in suprabasal layer (Fig. 4E); on day 5 (Fig. 4F) and day 7 (Fig. 4G), positive cells were located mainly in the stratum corneum. By day 14, GFP-positive cells had spread and merged with each other in the stratum corneum such that it was difficult to identify individual positive cells (Fig. 4H).

4. Discussion

This study was designed to investigate whether ultrasound with microbubble enhancement could efficiently transfer foreign genes into human LSE. We have shown that GFP plasmid DNA was efficiently delivered into the epidermis of the LSE. The transfected LSE graft survived on full-thickness wounds of nude mice and expressed the transgene for up to 2 weeks. Physical parameters are known to influence the efficiency of ultrasound-mediated gene transfection and the viability of the target cells [21]. Optimal conditions vary according to cell type and concentration, the size and composition of the microbubbles, and whether transfection is conducted in vivo or in vitro [19–21,25]. In the ex vivo LSE transfection experiments described here, a mixture of albumin-coated, octafluoropropane-gas-filled microbubbles (2.0–4.5 μm) and plasmid encoding GFP were applied to the dermal–epidermal junction of the LSE, which was then exposed to ultrasound under a variety of conditions. After testing several combinations of ultrasound parameters, i.e., frequency, intensity, and exposure duration, we found that an exposure of 2 Hz for 60 s at an intensity of 8 resulted in the efficient transfer of GFP plasmid DNA into the LSE epidermis. In another trial, keratinocytes (at different concentrations) in culture medium were mixed with the microbubbles and GFP plasmid DNA and then exposed to ultrasound. Contrary to our expectations, very few GFP-positive cells were obtained using either the optimal conditions for LSE described above or any other combination of exposure parameters (data not shown).

The combined use of microbubbles and ultrasound can greatly increase gene transfer efficiency [26], and the number of positively transduced cells

is further increased by repeated exposure to microbubble-mediated ultrasound [27]. In this study, multiple transfections were carried out, resulting in both multi-layer GFP expression and an increase in the number of epidermal cells expressing the transferred gene. These results indicate that re-transfection is another approach to increase transfection efficiency in LSEs.

It was observed that, in transfected LSEs, most of the GFP-positive cells migrated upward from the basal layer, both in culture and after transplantation. In the transfected LSEs transplanted onto nude mice, the positively transfected cells persisted, moving from the basal layer to the stratum corneum, until day 14 in stratum corneum and by day 21 almost all fluorescence was lost. This process coincided with one turnover time of the epidermis. In epidermis, most keratinocytes continue to differentiate and eventually slough off the skin surface, so that a gene transfected into these keratinocytes might eventually be lost. Nonetheless, transient transgene expression may play a role in supplementing growth factors and cytokines that are lacking in abnormalities linked to inadequate wound healing. For example, it has been reported that the transduction of hepatocyte growth factor into keratinocytes caused transient epidermal hyperproliferation in an LSE [28]. The mixture of GFP plasmid DNA and mibrobubble was administered at the dermal-epidermal junction of the LSEs, and then ultrasound was applied. We investigated the GFP expression in the peeled epidermis and the frozen sectioned collagen gel, respectively. By contrast to the epidermis, we rarely observed fluorescence-positive cells in the collagen gel (data not shown). Similar phenomenon was reported in in vivo or ex vivo gene delivery by intradermal injection, which was supposed due to the relatively fewer fibroblasts in the dermis or the inefficiency of the dermal cells to take-up and express the injected naked DNA [16].

To obtain sustained gene expression, gene transfer should be targeted to stem cells that possess unlimited growth potential and self-renewal capacity. Recent findings have suggested that integrin β1, integrin α6, CD 71, CD 34, keratin 15, keratin 19, and p63 can serve as epidermal stem cell markers [29–37], although none of these is sufficient to unambiguously identify stem cells in vivo. Until now, there have been few reports confirming the existence of stem cells in LSE constructed by seeding keratinocytes onto fibroblast-populated collagen gels. However, it is highly likely that stem cells are present in LSE as an Apligraf skin equivalent continued to survive on nude mice for over 1 year after transplantation [38] and transgene expression in keratinocytes transfected by lentiviral or retroviral vectors in skin equivalents was observed up to 13 weeks (4–6 epidermal turnovers) post-grafting [8].

Ultrasound with microbubble enhancement has proved to be effective as a non-viral gene transfer technique in many cell types in vivo and in vitro [19–22,39]. In addition, the mechanism of this technique in gene transfer [40,41] does not imply limitations in transferring foreign genes into either dividing or non-dividing cells. In this study, we found that some fluorescence-positive cells lagged behind others in their upward migration and that some remained in the basal layer as late as days 5–7 after gene transduction. These lagging or remaining cells might be transit-amplifying cells or stem cells. Among the 20–30 frozen slices prepared from samples taken on day 5 or 7 after transduction, only a few contained GFP-positive cells in the basal layer of the epidermis. Stem cells represent only a small portion of the basal cells in the interfollicular epidermis [42] and may be even less frequent in the LSE, as there is no stem cell influx from the multipotent stem cells lodged in the bulge areas of the hair follicles. However, keratinocyte progenitor cells or stem cells could be transfected using the ultrasound technique, implying that the number of stem cells thus transfected could be increased under more appropriate conditions and that sustained transgene expression could be expected.

In the ex vivo experiment described here, keratinocytes of LSEs were efficiently transfected with microbubble-enhanced ultrasound. The transfected LSEs that were subsequently transplanted onto nude mice survived well and continued to express the transgene. This proves not only that efficient gene transfer into human LSE can be obtained by this technique but also that the use of genetically modified LSE is a practical strategy in the treatment of cutaneous disorders.

Acknowledgements

This work was partly supported by Health Sciences Research Grants for Research on Specific Diseases from the Ministry of Health, Labor, and Welfare of Japan and a Grant-in-Aid for Scientific Research from the Ministry of Education, Culture, Sports, Science, and Technology of Japan.

References

[1] Waymack P, Duff RG, Sabolinski M, Kirsner RS. The Apligraf Burn Study Group. The effect of a tissue engineered bilayered living skin analog, over meshed split-thickness

autografts on the healing of excised burn wounds. The use of Apligraf in acute wounds. Burns 2000;26:609–19.
[2] Falanga V, Margolis D, Alvarez O, Auletta M, Maggiacomo F, Altman M, et al., Human Skin Equivalent Investigators Group. Rapid healing of venous ulcers and lack of clinical rejection with an allogeneic cultured human skin equivalent. Arch Dermatol 1998;134:293–300.
[3] Kirsner RS. The use of Apligraf in acute wounds. J Dermatol 1998;25:805–11.
[4] Andreadis ST. Gene transfer to epidermal stem cells: implications for tissue engineering. Expert Opin Biol Ther 2004; 4:783–800.
[5] Kaneda Y, Tamai K. Current status and future prospects of gene therapy technologies toward the treatment of intractable skin diseases. Arch Dermatol Res 2003;295:S63–6.
[6] Khavari PA, Rollman O, Vahlquist A. Cutaneous gene transfer for skin and systemic diseases. J Intern Med 2002;252:1–10.
[7] Ghazizadeh S, Harrington R, Garfield J, Taichman LB. Retrovirus-mediated transduction of porcine keratinocytes in organ culture. J Invest Dermatol 1998;111:492–6.
[8] Kuhn U, Terunuma A, Pfutzner W, Foster RA, Vogel JC. In vivo assessment of gene delivery to keratinocytes by lentiviral vectors. J Virol 2002;76:1496–504.
[9] Freiberg RA, Choate KA, Deng H, Alperin ES, Shapiro LJ, Khavari PA. A model of corrective gene transfer in X-linked ichthyosis. Hum Mol Genet 1997;6:927–33.
[10] Woodley DT, Keene DR, Atha T, Huang Y, Ram R, Kasahara N, et al. Intradermal injection of lentiviral vectors corrects regenerated human dystrophic epidermolysis bullosa skin tissue in vivo. Mol Ther 2004;10:318–26.
[11] Pislaru S, Janssens SP, Gersh BJ, Simari RD. Defining gene transfer before expecting gene therapy: putting the horse before the cart. Circulation 2002;106:631–6.
[12] Newman KD, Dunn PF, Owens JW, Schulick AH, Virmani R, Sukhova Q, et al. Adenovirus-mediated gene transfer into normal rabbit arteries results in prolonged vascular cell activation, inflammation, and neointimal hyperplasia. J Clin Invest 1995;96:2955–65.
[13] Fox JL. US authorities uphold suspension of SCID gene therapy. Nat Biotechnol 2003;21:217.
[14] Schmidt-Wolf GD, Schmidt-Wolf IG. Non-viral and hybrid vectors in human gene therapy: an update. Trends Mol Med 2003;9:67–72.
[15] Vogel JC. Non-viral skin gene therapy. Hum Gene Ther 2000;11:2253–9.
[16] Hengge UR, Walker PS, Vogel JC. Expression of naked DNA in human, pig, and mouse skin. J Clin Invest 1996;97: 2911–6.
[17] Hengge UR, Chan EF, Foster RA, Walker PS, Vogel JC. Cytokine gene expression in epidermis with biological effects following injection of naked DNA. Nat Genet 1995;10: 161–6.
[18] Sawamura D, Meng X, Ina S, Sato M, Tamai K, Hanada K, et al. Induction of keratinocyte proliferation and lymphocytic infiltration by in vivo introduction of the IL-6 gene into keratinocytes and possibility of keratinocyte gene therapy for inflammatory skin diseases using IL-6 mutant genes. J Immunol 1998;161:5633–9.
[19] Lawrie A, Brisken AF, Francis SE, Wyllie D, Kiss-Toth E, Qwarnstrom EE, et al. Ultrasound-enhanced transgene expression in vascular cells is not dependent upon cavitation-induced free radicals. Ultrasound Med Biol 2003;29:1453–61.
[20] Li T, Tachibana K, Kuroki M. Gene transfer with echo-enhanced contrast agents: comparison between albunex, optison, and levovist in mice-initial results. Radiology 2003;229:423–8.
[21] Zarnitsyn VG, Prausnitz MR. Physical parameters influencing optimization of ultrasound-mediated DNA transfection. Ultrasound Med Biol 2004;30:527–38.
[22] Lawrie A, Brisken AF, Francis SE, Tayler DI, Chamberlain J, Crossman DC, et al. Ultrasound enhances reporter gene expression after transfection of vascular cells in vitro. Circulation 1999;99:2617–20.
[23] Shirakata Y, Tokumaru S, Yamasaki K, Sayama K, Hashimoto K. So-called biological dressing effects of cultured epidermal sheets are mediated by the production of EGF family. TGF-beta and VEGF. J Dermatol Sci 2003;32:209–15.
[24] Shirakata Y, Ueno H, Hanakawa Y, Kameda K, Yamasaki K, Tokumaru S, et al. TGF-beta is not involved in early phase growth inhibition of keratinocytes by 1alpha, 25(OH)2vitamin D3. J Dermatol Sci 2004;36:41–50.
[25] Chen S, Shohet RV, Bekeredjian R, Frenkel P, Grayburn PA. Optimization of ultrasound parameters for cardiac gene delivery of adenoviral or plasmid deoxyribonucleic acid by ultrasound-targeted microbubble destruction. J Am Coll Cardiol 2003;42:301–8.
[26] Lawrie A, Brisken AF, Francis SE, Cumberland DC, Crossman DC, Newman CM. Microbubble-enhanced ultrasound for vascular gene delivery. Gene Ther 2000;7:2023–7.
[27] Bekeredjian R, Chen S, Frenkel PA, Grayburn PA, Shohet RV, Frenkel P. Ultrasound-targeted microbubble destruction can repeatedly direct highly specific plasmid expression to the heart Optimization of ultrasound parameters for cardiac gene delivery of adenoviral or plasmid deoxyribonucleic acid by ultrasound-targeted microbubble destruction. Circulation 2003;108:1022–6.
[28] Hamoen KE, Morgan JR. Transient hyperproliferation of a transgenic human epidermis expressing hepatocyte growth factor. Cell Transplant 2002;11:385–95.
[29] Bickenbach JR. Isolation, characterization, and culture of epithelial stem cells. Meth Mol Biol 2005;289:97–102.
[30] Gambardella L, Barrandon Y. The multifaceted adult epidermal stem cell. Curr Opin Cell Biol 2003;15:771–7.
[31] Koster MI, Roop DR. The role of p63 in development and differentiation of the epidermis. J Dermatol Sci 2004;34: 3–9.
[32] Larouche D, Hayward C, Cuffley K, Germain L. Keratin 19 as a stem cell marker in vivo and in vitro. Meth Mol Biol 2005;289:103–10.
[33] Lavker RM, Sun TT. Epidermal stem cells: properties, markers, and location. Proc Natl Acad Sci USA 2000;97: 13473–5.
[34] Radu E, Simionescu O, Regalia T, Dumitrescu D, Popescu LM. Stem cells (p63(+)) in keratinocyte cultures from human adult skin. J Cell Mol Med 2002;6:593–8.
[35] Trempus CS, Morris RJ, Bortner CD, Cotsarelis Q, Faircloth RS, Reece JM, et al. Enrichment for living murine keratinocytes from the hair follicle bulge with the cell surface marker CD34. J Invest Dermatol 2003;120:501–11.
[36] Watt FM. The stem cell compartment in human interfollicular epidermis. J Dermatol Sci 2002;28:173–80.
[37] Webb A, Li A, Kaur P. Location and phenotype of human adult keratinocyte stem cells of the skin. Differentiation 2004; 72:387–95.
[38] Guerret S, Govignon E, Hartmann DJ, Ronfard V. Long-term remodeling of a bilayered living human skin equivalent (Apligraf) grafted onto nude mice: Immunolocalization of human cells and characterization of extracellular matrix. Wound Repair Regen 2003;11:35–45.
[39] Endoh M, Koibuchi N, Sato M, Morishita R, Kanzaki T, Murata Y, et al. Fetal gene transfer by intrauterine injection with microbubble-enhanced ultrasound. Mol Ther 2002;5:501–8.

[40] Tachibana K, Uchida T, Ogawa K, Yamashita N, Tamura K. Induction of cell-membrane porosity by ultrasound. Lancet 1999;353:1409.
[41] Dijkmans PA, Juffermans LJ, Musters RJ, van Wamel A, ten Cate FJ, van Gilst W, et al. Microbubbles and ultrasound: From diagnosis to therapy. Eur J Echocardiogr 2004;5:245–56.
[42] Li A, Simmons PJ, Kaur P. Identification and isolation of candidate human keratinocyte stem cells based on cell surface phenotype. Proc Natl Acad Sci USA 1998;95:3902–7.

Induction of Keratinocyte Migration via Transactivation of the Epidermal Growth Factor Receptor by the Antimicrobial Peptide LL-37[1]

Sho Tokumaru,[2]* Koji Sayama,[2,3]* Yuji Shirakata,* Hitoshi Komatsuzawa,† Kazuhisa Ouhara,† Yasushi Hanakawa,* Yoko Yahata,* Xiuju Dai,* Mikiko Tohyama,* Hiroshi Nagai,* Lujun Yang,* Shigeki Higashiyama,‡ Akihiko Yoshimura,§ Motoyuki Sugai,† and Koji Hashimoto*

The closure of skin wounds is essential for resistance against microbial pathogens, and keratinocyte migration is an important step in skin wound healing. Cathelicidin hCAP18/LL-37 is an innate antimicrobial peptide that is expressed in the skin and acts to eliminate microbial pathogens. Because hCAP18/LL-37 is up-regulated at skin wound sites, we hypothesized that LL-37 induces keratinocyte migration. In this study, we found that 1 μg/ml LL-37 induced the maximum level of keratinocyte migration in the Boyden chamber assay. In addition, LL-37 phosphorylated the epidermal growth factor receptor (EGFR) after 10 min, which suggests that LL-37-induced keratinocyte migration occurs via EGFR transactivation. To test this assumption, we used inhibitors that block the sequential steps of EGFR transactivation, such as OSU8-1, CRM197, anti-EGFR no. 225 Ab, and AG1478. All of these inhibitors completely blocked LL-37-induced keratinocyte migration, which indicates that migration occurs via HB-EGF-mediated EGFR transactivation. Furthermore, CRM197, anti-EGFR no. 225, and AG1478 blocked the LL-37-induced phosphorylation of STAT3, and transfection with a dominant-negative mutant of STAT3 abolished LL-37-induced keratinocyte migration, indicating the involvement of the STAT3 pathway downstream of EGFR transactivation. Finally, we tested whether the suppressor of cytokine signaling (SOCS)/cytokine-inducible Src homology 2-containing protein (CIS) family of negative regulators of STAT3 regulates LL-37-induced keratinocyte migration. Transfection with SOCS1/Jak2 binding protein or SOCS3/CIS3 almost completely abolished LL-37-induced keratinocyte migration. In conclusion, LL-37 induces keratinocyte migration via heparin-binding-EGF-mediated transactivation of EGFR, and SOCS1/Jak 2 binding and SOCS3/CIS3 negatively regulate this migration. The results of this study suggest that LL-37 closes skin wounds by the induction of keratinocyte migration. *The Journal of Immunology,* **2005, 175: 4662–4668.**

Antimicrobial peptides are short amino acid sequences that can kill a variety of microbial pathogens. The major human antimicrobial peptides are the defensins and cathelicidin (1–4). Defensins are cysteine-rich cationic peptides and are further classified as α- or β-defensins based on structure. The α-defensins 1–4 (HNP1–4) are produced by neutrophils (5, 6), and the α-defensins 5 and 6 are found in Paneth cells of the gastrointestinal tract (7, 8). The β-defensins 1–4 (hBD 1–4)[4] are produced by epithelial tissues (9–12). hCAP18/LL-37 is the only human antimicrobial peptide that has been identified as a member of the cathelicidin family; it is produced in many tissues and cell types (4) and is processed to LL-37 in neutrophils (13). In the skin, epidermal keratinocytes produce hBD1–4 and hCAP18/LL-37 (4, 9–12). Murakami (14) analyzed sweat samples and identified three additional forms of cathelicidin peptide which deliver innate effector molecules in the absence of inflammation. Mast cells in the dermis were also found to produce hCAP18/LL-37 (15).

The epidermis plays an essential role in resistance against microbial-borne disease, as it is constantly exposed to a variety of microbial pathogens. The hBDs and hCAP18/LL-37 play major roles in this innate immune system (16). In addition, the epidermis functions as a physical barrier to microbial pathogens. However, once this physical barrier is disrupted by wounding, microbial pathogens can invade the underlying tissue. Therefore, the efficient closure of skin wounds is vital to the maintenance of homeostasis. In contrast, wounded skin expresses antimicrobial peptides, such as hCAP18/LL-37 and defensins (17–19). Although antimicrobial peptides were originally identified as molecules that kill microbial pathogens, there is strong evidence that these peptides have functions in antimicrobial immunity other than direct antimicrobial activity.

*Department of Dermatology, Ehime University School of Medicine, Ehime, Japan; †Department of Bacteriology, Hiroshima University Graduate School of Biomedical Sciences, Hiroshima, Japan; ‡Department of Molecular and Cellular Biology, Division of Biochemistry and Molecular Genetics, Ehime University School of Medicine, Ehime, Japan; and §Division of Molecular and Cellular Immunology, Medical Institute of Bioregulation, Kyushu University, Fukuoka, Japan

Received for publication March 10, 2005. Accepted for publication July 22, 2005.

The costs of publication of this article were defrayed in part by the payment of page charges. This article must therefore be hereby marked *advertisement* in accordance with 18 U.S.C. Section 1734 solely to indicate this fact.

[1] This work was supported by grants from the Ministries of Health, Labor, and Welfare and Education, Culture, Sports, Science, and Technology of Japan.

[2] S.T. and K.S. contributed equally to this article.

[3] Address correspondence and reprint requests to Dr. Koji Sayama, Department of Dermatology, Ehime University School of Medicine, Toon-City, Ehime 791-0295, Japan. E-mail address: sayama@m.ehime-u.ac.jp

[4] Abbreviations used in this paper: hBD, β-defensin; EGF, epidermal growth factor; EGFR, EGF receptor; HB-EGF, heparin-binding EGF; BHE, bovine hypothalamic extract; Ax, adenovirus vector; JAB, Jak2 binding; moi, multiplicity of infection; SOCS, suppressor of a cytokine signaling; CIS, cytokine-inducible Src homology 2-containing protein; STAT3F, dominant-negative mutants of STAT3; fPRL-1, formyl peptide receptor-like 1.

0022-1767/05/$02.00

Recently, it was revealed that these antimicrobial peptides are multifunctional proteins (20). Although hBDs are chemotactic for dendritic cells, LL-37 is chemotactic for neutrophils, monocytes, and T cells, but not for dendritic cells (3, 21, 22). LL-37 modulates dendritic cell differentiation and promotes Th1 responses (23). In the case of endothelial cells, LL-37 induces angiogenesis that is mediated by the formyl peptide receptor-like 1 receptor (24). In wounded skin, hCAP18/LL-37 is up-regulated, whereas the hCAP18/LL-37 levels in chronic ulcers are low (19). Furthermore, anti-LL-37 Ab inhibits re-epithelialization of skin wounds (19). These findings suggest that, apart from having antimicrobial activity, LL-37 plays an important role in wound healing.

The migration of epidermal keratinocytes is an important step in skin wound healing. Growth factors and the epidermal growth factor (EGF) receptor (EGFR) are involved in keratinocyte migration and proliferation (25, 26). Extracellular stimuli from the EGF and non-EGF families can activate the EGFR. These diverse stimuli include numerous agonists for heptahelical G-protein-coupled receptors, cytokines, and integrins (27, 28). The activation of the EGFR by non-EGFR ligands is called transactivation (27) and is mediated, at least in part, by heparin-binding EGF (HB-EGF), which is cleaved from its membrane-anchored form (pro-HB-EGF) by a specific metalloproteinase (29, 30). Recently, the transactivation of EGFR by LL-37 was reported for airway epithelial cells (31), which suggests that LL-37 induces keratinocyte migration via EGFR transactivation during skin wound healing.

The intracellular signaling molecule, STAT3, is involved in keratinocyte migration (32). The STAT family consists of STATs 1, 2, 3, 4, 5a, 5b, and 6. STATs and adaptor molecules are sequentially activated upon the binding of a cytokine to its receptor. After phosphorylation, STAT forms a homodimer or heterodimer, translocates into the nucleus, and initiates the transcription of target genes (33). These STAT signaling pathways are negatively regulated by the suppressor of a cytokine signaling (SOCS)/cytokine-inducible Src homology 2-containing protein (CIS) family, thereby avoiding oversignaling (34). In human keratinocytes, SOCS3/CIS3 negatively regulates hepatocyte growth factor-induced migration (35). Therefore, the STAT3-SOCS/CIS family may also be involved in LL-37-induced keratinocyte migration.

In this study, we demonstrate that LL-37 induces keratinocyte migration, and we examine the molecular mechanisms underlying EGFR transactivation.

Materials and Methods

Synthesis of LL-37

LL-37 was synthesized using a peptide synthesizer (Shimazu), as described previously (36). The peptide was purified using reverse-phase HPLC with an octadecyl-4PW column (Tosoh) and a linear gradient of aqueous 0.05% trifluoroacetic acid to 100% acetonitrile that contained 0.05% trifluoroacetic acid, and the sample was then lyophilized to remove the organic solvent. To confirm peptide purity and quality, mass spectrometry using the MALDI/TOF-mass spectrometry method was performed with Voyager (PerSeptive Biosystems). The peptides were assayed for LPS contamination by the *Limulus* test (Seikagaku).

Reagents and Abs

The following Abs were used: STAT3 (clone 84; BD Transduction Laboratories), phospho-STAT3 (no. 9131; Cell Signaling Technology), EGFR (clone 13; BD Transduction Laboratories), and phospho-EGFR (clone 9H2; Upstate Biotechnology) and EGFR neutralizing Ab (clone 225; Oncogene Research Products). AG1478 and CRM197 were purchased from Merck. OSU8–1 (37) was a gift from Canebo Science.

Keratinocyte culture

Primary normal human keratinocytes were isolated from normal human skin and cultured as previously described (38). The human skin samples were obtained after plastic surgery under a protocol approved by the Institutional Review Board of Ehime University School of Medicine. The skin samples were cut into 3- to 5-mm pieces and incubated with 250 U/ml dispase (Godoshusei) in DMEM overnight at 4°C. After separation of the epidermis from the dermis, the epidermal sheets were incubated in a 0.25% trypsin solution for 10 min at 37°C and teased with forceps. The keratinocytes were collected by centrifugation and were further cultured in MCDB153 medium that was supplemented with insulin (1 μg/ml), hydrocortisone (0.5 μM), ethanolamine (0.1 mM), phosphoethanolamine (0.1 mM), bovine hypothalamic extract (BHE; 50 μg/ml), and Ca^{2+} (0.1 mM). This supplement has been described elsewhere (39).

Migration assay

Keratinocyte migration was assayed quantitatively with a Boyden chamber, as described previously (40). Designated amounts of LL-37 were added to the bottom wells of a 48-well Boyden chamber (Neuro Probe), and an 8-μm pore-size polyvinylpyrrolidone-free polycarbonate membrane (Neuro Probe) was placed on the wells. The membrane was precoated with type I collagen (10 μg/ml in PBS; Nitta Gelatin) at room temperature for 1 h and then washed extensively with PBS. Subconfluent keratinocytes were harvested with trypsin-EDTA (0.05% trypsin and 0.5 mM EDTA) and resuspended in culture medium without BHE at 1×10^5 cells/ml. A 50-μl aliquot of the keratinocyte suspension (5,000 cells/well) was added to the upper wells, and the chamber was incubated overnight at 37°C in a humidified atmosphere of air with 5% CO_2. The cells that adhered to the upper surface of the filter membrane were removed by scraping with a rubber blade, and the cells that moved through the filter and stayed on the lower surface of the membrane were considered to be migrated cells. The membrane was fixed with 10% buffered formalin overnight and then stained overnight with Gill's hematoxylin. The membrane was then mounted between two glass slides with 90% glycerol, and the number of migrated cells was determined by counting under a microscope.

The role of EGFR transactivation in LL-37-induced keratinocyte migration was analyzed by the inhibition of EGFR transactivation with OSU8-1 (37), anti-EGFR neutralizing Ab no. 225, CRM197 (37), and AG1478. OSU8-1 (1 μM), anti-EGFR no. 225 (10 μg/ml), CRM197 (1 μg/ml), and AG1478 (30 nM) were added to the lower chamber together with 1 μg/ml LL-37, and LL-37-induced keratinocyte migration was analyzed as described previously.

Western blotting

Subconfluent keratinocytes were starved for 2 h in BHE-free medium and then stimulated with LL-37 as indicated. The cells were harvested on ice in lysis buffer that contained 5 mM EDTA, 100 μM sodium orthovanadate, 100 μM sodium pyrophosphate, 1 mM sodium fluoride, 5 μM 3,4-dichloroisocumarin, 1 μg/ml aprotinin, and 1% Triton X-100 in PBS. A 20-μg sample of protein was separated on 10% SDS-PAGE and then transferred to a polyvinylidene difluoride membrane. The membranes were blocked overnight at 4°C with 5% skimmed milk in PBS. The blocked membranes were incubated for 6 h with the first Ab as indicated. After three washes with PBS that contained 0.05% Tween 20, the membranes were treated with ABC reagents (Vector Laboratories) for 20 min at room temperature, washed three times with PBS that contained 0.05% Tween 20, treated with ECL detection reagents (Amersham Pharmacia Biotech) for 1 min at room temperature, and exposed to photographic film (Kodak).

Adenovirus vectors (Axs)

STAT3 has a phosphorylation site at tyrosine 705. In dominant-negative mutants of STAT3 (STAT3F), the phosphorylatable tyrosine residues are substituted with phenylalanine. Axs that encode STAT3F (AxCAStat3F), SOCS1/Jak2-binding (JAB) (AxCAJAB), and SOCS3/CIS3 (AxCACIS3) were generated as described previously (41), using the cosmid cassettes and Ad DNA-terminal protein complex method (42). An Ax that encodes lacZ (Ax LacZ) was a gift from Dr. I. Saito (University of Tokyo, Tokyo, Japan). Virus stocks were prepared using a standard procedure (42). Concentrated, purified virus stocks were prepared using a CsCl gradient, and the virus titer was checked using a plaque formation assay. We infected normal human keratinocytes with Axs at a multiplicity of infection (moi) of 5.

Statistical analyses

Data were collected from at least three independent experiments. Quantitative data are expressed as the mean ± SE. Statistical significance was determined by the paired Student *t* test. Differences were considered to be statistically significant for $p < 0.05$. The levels of statistical significance are indicated in the figures as follows: *, $p < 0.05$; **, $p < 0.01$.

Results

LL-37 induces keratinocyte migration

Initially, we investigated whether LL-37 induced keratinocyte migration. After the addition of 1 μg/ml LL-37 to cultured normal human keratinocytes, cell migration was observed by phase contrast microscopy. LL-37 induced keratinocyte migration at 12 h compared with the control (Fig. 1*A*). Next, we quantitatively analyzed LL-37-induced migration using the Boyden chamber assay (Fig. 1*B*). Various amounts of LL-37 and cultured keratinocytes were added to the lower and upper chambers, respectively. After incubation overnight, the migrated keratinocytes were counted. LL-37 induced a 3-fold increase in keratinocyte migration compared with the control treatment. The optimum concentration of LL-37 to induce migration was 1 μg/ml.

LL-37 phosphorylates EGFR

Because EGFR is involved in keratinocyte migration, we investigated whether EGFR transactivation is involved in LL-37-induced keratinocyte migration by analyzing the phosphorylation of EGFR by LL-37 (Fig. 2). LL-37 phosphorylated EGFR at 10 min, and the phosphorylation persisted for 15 min. The amount of EGFR protein did not change during this time period.

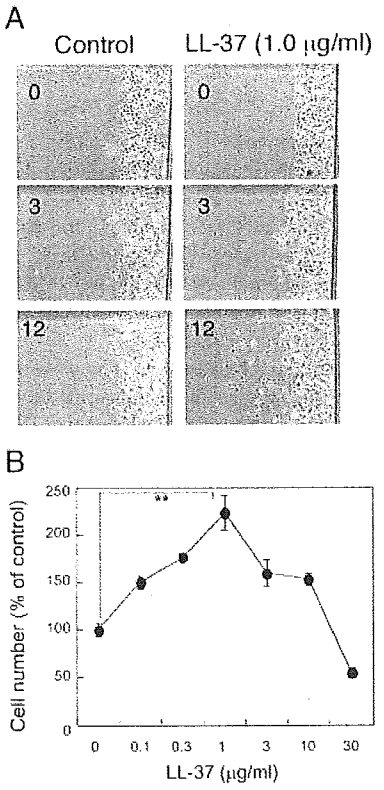

FIGURE 1. LL-37-induced keratinocyte migration. *A*, Keratinocyte migration was observed under the phase contrast microscope. A portion of the keratinocytes was removed from the tissue culture plates by scraping, and the remaining cells were cultured further with 1 μg/ml LL-37. The levels of cell migration were observed at 3 and 12 h. *B*, Keratinocyte migration was assayed quantitatively using the Boyden chamber. The indicated amounts of LL-37 were added to the bottom wells of a 48-well Boyden chamber, and an 8-μm pore-size polyvinylpyrrolidone-free polycarbonate membrane was placed on the wells. Keratinocytes were added to the upper wells at 5000 cells/well. After overnight incubation, the membrane was stained with Gill's hematoxylin. The number of cells that had migrated through the filter was determined by counting under a microscope. The data are shown as percentages of the control migration. Each point shows the mean ± SD of quadruplicate measurements. **, $p < 0.01$.

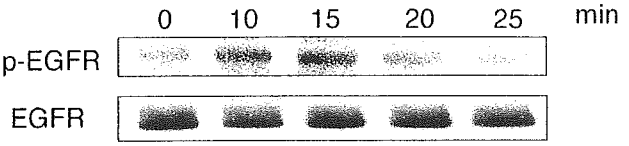

FIGURE 2. Activation of EGFR by LL-37. Phosphorylation of EGFR by LL-37. Subconfluent keratinocytes were starved for 2 h in BHE-free medium and stimulated with 1 μg/ml LL-37. The cells were harvested into lysis buffer at the indicated times. The phosphorylation of EGFR (p-EGFR) was analyzed by Western blotting. EGFR indicates total EGFR protein.

LL-37-induced keratinocyte migration occurs via HB-EGF-mediated EGFR transactivation

The activation of EGFR suggests that LL-37-induced keratinocyte migration is via EGFR transactivation. To confirm this suggestion, we used several inhibitors that block the sequential steps of EGFR transactivation (Figs. 3 and 4*B*). In EGFR transactivation, extracellular stimuli activate a metalloproteinase on the cell membrane, which cleaves the extracellular domain of the EGF family. The cleaved EGF then binds and phosphorylates EGFR, which transduces the signals into the intracellular signaling pathways. OSU8-1 is a metalloproteinase inhibitor that blocks the shedding of EGF family members (37). CRM197 is a nontoxic mutant of diphtheria toxin that binds to the extracellular domain of the membrane-anchored form of HB-EGF and inhibits the soluble form of HB-EGF, whereas it does not bind to other EGF family members, such as

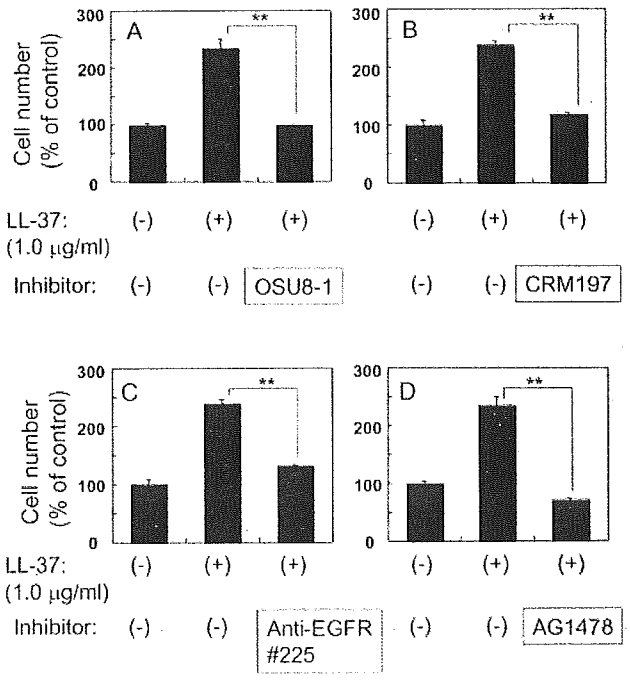

FIGURE 3. Inhibition of LL-37-induced keratinocyte migration by OSU8-1, CRM197, anti-EGFR no. 225, and AG1478. In the presence of inhibitors of EGFR transactivation, LL-37-induced keratinocyte migration was analyzed in the Boyden chamber assay. The mechanisms of action of these inhibitors are shown in Fig. 7. OSU8-1 (1 μM), CRM197 (1 μg/ml), anti-EGFR no. 225 (10 μg/ml), and AG1478 (30 nM) (*A–D*, respectively) were added to the lower chamber together with 1.0 μg/ml LL-37, and LL-37-induced keratinocyte migration was analyzed as described in Fig. 1. **, $p < 0.01$.

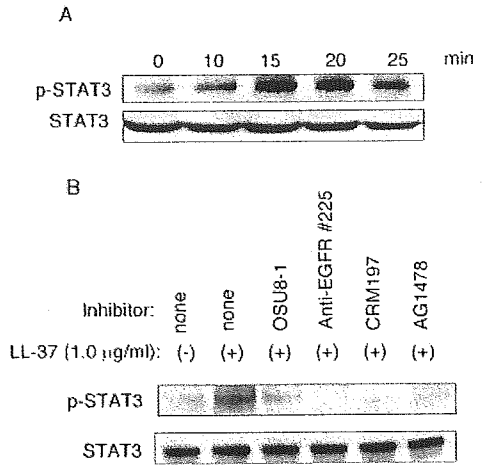

FIGURE 4. Phosphorylation of STAT3 by LL-37. *A*, Phosphorylation of STAT3 by LL-37. Subconfluent keratinocytes were starved for 2 h in BHE-free medium, and stimulated with 1 μg/ml LL-37. The cells were harvested into lysis buffer at the indicated time. The phosphorylation of STAT3 (p-STAT3) was analyzed by Western blotting. STAT3 indicates total STAT3 protein. *B*, Inhibition of LL-37-induced STAT3 phosphorylation by OSU8-1, anti-EGFR no. 225, CRM197, and AG1478. Keratinocytes were pretreated with OSU8-1 (1 μM), anti-EGFR no. 225 (10 μg/ml), CRM197 (1 μg/ml), or AG1478 (30 nM) for 1 h and then stimulated with 1 μg/ml LL-37 for 15 min. The phosphorylation of STAT3 was analyzed by Western blotting.

EGF, TGF-α, amphiregulin, and betacellulin (37). The anti-EGFR no. 225 Ab blocks the binding of EGF family members to the EGFR. AG1478 is an inhibitor of EGFR tyrosine kinase, which blocks the activation of EGFR.

Using these inhibitors, we investigated whether the inhibition of EGFR transactivation blocks LL-37-induced keratinocyte migration. After the addition of OSU8-1, CRM197, anti-EGFR no. 225, and AG1478 to the lower chamber with LL-37, keratinocyte migration was analyzed quantitatively using the Boyden chamber, as shown in Fig. 1. All of the inhibitors, including OSU8-1, CRM197, anti-EGFR no. 225, and AG1478, completely blocked LL-37-induced keratinocyte migration (Fig. 3). As LL-37 phosphorylates EGFR, and because LL-37-induced migration was completely blocked by OSU8-1, CRM197, anti-EGFR no. 225, and AG1478, we conclude that LL-37-induced keratinocyte migration is via HB-EGF-mediated EGFR transactivation.

LL-37 phosphorylates STAT3 via HB-EGF-mediated EGFR transactivation

A previous study has demonstrated that the STAT3 signaling pathway is involved in keratinocyte migration (32). Therefore, we studied the involvement of STAT3 in LL-37-induced keratinocyte migration. LL-37 maximally phosphorylated STAT3 at 15 min as determined by densitometric analysis, and the level of phosphorylation decreased at 25 min (Fig. 4). The amount of STAT3 protein did not change during this time. We also investigated whether LL-37-induced STAT3 phosphorylation occurred via HB-EGF-mediated EGFR transactivation. Keratinocytes were pretreated with OSU8-1, CRM197, anti-EGFR no. 225, and AG1478 for 1 h and were then stimulated with LL-37 for 15 min, followed by Western blot analysis. All of these inhibitors blocked LL-37-induced STAT3 phosphorylation, which again indicates that LL-37-induced STAT3 phosphorylation is via HB-EGF-mediated EGFR transactivation.

STAT3 is essential for LL-37-induced keratinocyte migration

We investigated whether STAT3 is essential for LL-37-induced keratinocyte migration. We constructed dominant-negative mutants of STAT3 (STAT3F) as well as Ax-carrying STAT3F (AxCAStat3F), as described previously (41). AxCAStat3F and the control vector AxLacZ were transfected (moi = 10) into keratinocytes. The expression of STAT3F almost completely blocked both LL-37-induced STAT3 phosphorylation and LL-37-induced keratinocyte migration (Fig. 5). Because STAT3 was phosphorylated by LL-37 and LL-37-induced migration was blocked by STAT3F, we conclude that the phosphorylation of STAT3 is essential for LL-37-induced keratinocyte migration.

SOCS1/JAB and SOCS3/CIS3 inhibit LL-37-induced keratinocyte migration

Because STAT3 is involved in LL-37-induced keratinocyte migration (as shown in Figs. 4 and 5), we analyzed the mechanism of regulation of STAT3 by SOCS1/JAB and SOCS3/CIS3. After the transfection of keratinocytes with AxCAJAB or AxCACIS3, LL-37-induced keratinocyte migration was analyzed quantitatively using the Boyden chamber assay (Fig. 6). The expression of either SOCS1/JAB or SOCS3/CIS3 almost completely blocked LL-37-induced keratinocyte migration. LL-37 induced neither SOCS1/JAB nor SOCS3/CIS3 (data not shown).

Discussion

The molecular mechanisms underlying LL-37-induced keratinocyte migration are summarized in Fig. 7. LL-37 activates the metalloproteinase, which cleaves the extracellular domain of HB-EGF. The soluble form of HB-EGF then binds to and phosphorylates EGFR. This, in turn, transduces the signals into the intracellular signaling pathways. STAT3 mediates this signaling pathway, leading to keratinocyte migration. SOCS1/JAB or SOCS3/CIS3 negatively regulates this STAT3 pathway and migration.

In a previous study, Tjabringa et al. (31) have shown that LL-37 activates airway epithelial cells, as demonstrated by its ability to activate ERK1/2 and to increase the release of IL-8. This activation

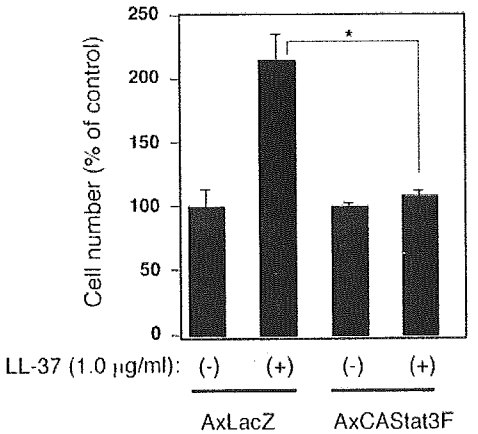

FIGURE 5. Inhibition of LL-37-induced keratinocyte migration by STAT3F. Ax LacZ and AxCAStat3F were transfected into normal human keratinocytes at a moi of 5. After 24 h, the keratinocytes were harvested and transferred to the upper well of the Boyden chamber. Then, 1 μg/ml LL-37 was added to the lower chamber, and keratinocyte migration was analyzed as described in Fig. 1. The numbers of migrated cells are shown as percentages of the control migration. Each point shows the mean ± SD of quadruplicate measurements. *, $p < 0.05$.

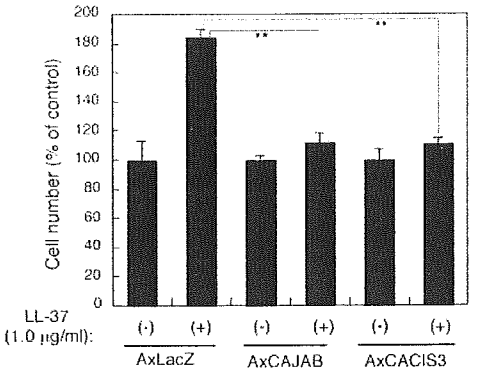

FIGURE 6. Inhibition of LL-37-induced keratinocyte migration by SOCS1/JAB and SOCS3/CIS3. Ax LacZ, AxCAJAB, and AxCACIS3 were transfected into normal human keratinocytes at a moi of 5. After 24 h, the keratinocytes were harvested and transferred to the upper well of the Boyden chamber. Then, 1 μg/ml LL-37 was added to the lower chamber, and keratinocyte migration was analyzed as described in Fig. 1. The numbers of migrated cells are shown as percentages of the control migration. Each point shows the mean ± SD of quadruplicate measurements. **, $p < 0.01$.

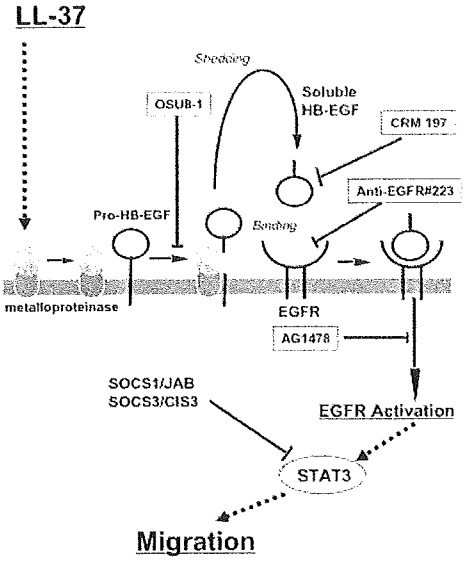

FIGURE 7. Proposed molecular mechanism of LL-37-induced keratinocyte migration. This scheme summarizes the pathway from LL-37 to keratinocyte migration and includes EGFR transactivation and STAT3. LL-37 activates the metalloproteinase, which cleaves the extracellular domain of HB-EGF. The soluble form of HB-EGF then binds and phosphorylates EGFR, which transduces the signals into the intracellular signaling pathways. OSU8-1 is a metalloproteinase inhibitor that blocks the shedding of EGF family proteins. CRM197 is a nontoxic mutant of diphtheria toxin that binds to the extracellular domain of the membrane-anchored form of HB-EGF; it inhibits the soluble form of HB-EGF but does not bind to the other EGF family members. The anti-EGFR no. 225 Ab blocks the binding of EGF family members to the EGFR. AG1478 is an inhibitor of EGFR tyrosine kinase, which blocks the activation of EGFR. OSU8-1, CRM197, anti-EGFR no. 225, and AG1478 all block LL-37-induced phosphorylation of EGFR and keratinocyte migration (Figs. 2 and 3), which indicates that the LL-37-induced EGFR activation occurs via HB-EGF-mediated EGFR transactivation. Following EGFR activation, keratinocyte migration is induced via STAT3 phosphorylation. SOCS1/JAB and SOCS3/CIS3 negatively regulate this STAT3 pathway.

requires the tyrosine kinase activity of the EGFR and involves the action of metalloproteinases and EGFR ligands, which indicates that the transactivation of EGFR is involved in this activation. The mechanism of this activation is quite similar to that of keratinocytes (Fig. 7). However, among the several EGFR ligands, no specific EGFR ligand for the transactivation of EGFR has been identified in airway epithelial cells. In keratinocytes, we found that HB-EGF is a mediator for LL-37-induced EGFR transactivation. The mechanism through which LL-37 activates metalloproteinase is still unclear. Several candidate molecules for the LL-37 receptor have been suggested, including the G protein-coupled formyl peptide receptor-like 1 (fPRL-1) (22, 24) and P2X7 (43). However, in airway epithelial cells, the activation was not inhibited by pertussis toxin or fPRL-1-antagonistic peptide, which indicates that fPRL-1 is not involved in transactivation of EGFR (31). Similarly, in keratinocytes, pertussis toxin did not inhibit LL-37-induced EGFR phosphorylation (data not shown), which suggests that fPRL-1 is not involved in LL-37-induced EGFR transactivation of keratinocytes. More recently, it has been suggested that LL-37 is able to cross the keratinocyte cell membrane and enter the cell (44). In this model, specific receptors are not required, and LL-37 may interact directly with the keratinocyte plasma membrane to cause conformational changes that activate indirectly a surface receptor that is linked to intracellular signaling molecules. If this is the case, it is possible that other highly cationic antimicrobial peptides, such as hBD1–3, also activate EGFR in keratinocytes. We tested this possibility and found that hBD1–3 phosphorylated EGFR in keratinocytes which suggests that the activation of keratinocytes is not unique to LL-37 among the antimicrobial peptides (our unpublished data).

The innate immune system is the first line of defense against microbial pathogens. Keratinocytes form a multilayered epidermis that separates the inner body from the outer environment and protects against a variety of microbial pathogens. Because the epidermis is the outermost layer of the body, epidermal keratinocytes are thought to be important components of innate immunity. Once the epidermis is disrupted by wounding, microbial pathogens can easily invade the body. Therefore, wound closure is an important issue for keratinocytes as participants in innate immunity. In this study, we have clearly demonstrated that LL-37 induces keratinocyte migration via EGFR transactivation. In the epidermis, bacterial contact, inflammation, and wounding are reported to stimulate keratinocytes to produce hCAP18/LL-37 (18, 36, 45). In addition to keratinocytes, granulocytes and skin mast cells produce hCAP18/LL-37 (4, 15). As hCAP18/LL-37 is up-regulated at the skin wound site (18), the present report strongly suggests that LL-37 induces keratinocyte migration to close the skin wound. In addition to its effects on keratinocytes, LL-37 can act on endothelial (24) and inflammatory cells, including neutrophils, monocytes, and T cells (22). Therefore, LL-37 may regulate skin wound healing through mechanisms that act directly on the cells within the wound environment rather than acting solely against microbial pathogens. Thus, hCAP18/LL-37 is a multifunctional mediator of innate immunity because it links host defenses and wound healing.

In the present study, the optimal concentration of LL-37 that induced keratinocyte migration was 1 μg/ml. The concentration of hCAP18/LL-37 at surgical wound sites has been reported to be ~2 μg/mg protein (19). Assuming that the protein concentration is similar to that in the serum (~70 mg/ml), the estimated concentration of hCAP18/LL-37 is 0.03 μg/ml. According to the data shown in Fig. 1, this concentration is insufficient to induce keratinocyte migration. However, immunohistochemical analysis has revealed that hCAP18/LL-37 is up-regulated, especially at the wound edge (19), which suggests that the local concentration of

LL-37 at the wound edge, where keratinocytes are migrating, may be high enough to induce migration.

Although we have shown that LL-37 induces keratinocyte migration, it has been reported that human serum inhibits the antimicrobial activity of LL-37 (46), which raises the possibility that serum also inhibits LL-37-induced keratinocyte migration during wound healing in vivo. In an ex vivo wound healing model, re-epithelialization occurred in two steps without inflammation, i.e., simple migration and subsequent proliferation of keratinocytes to form a provisional neoepidermis (19). Our data indicate that endogenous LL-37 mediates this keratinocyte migration. This ex vivo wound healing model requires medium that contains at least 10% FBS for re-epithelialization (47, 48). Furthermore, this re-epithelialization is inhibited by anti-LL-37 Ab (19), which indicates that endogenous LL-37 is a mediator of re-epithelialization even in the presence of serum. In addition to the ex vivo wound healing model, LL-37-induced migration of leukocytes is independent of the presence of serum (22). Therefore, LL-37-induced keratinocyte migration may not be hindered by the presence of serum or wound fluid in vivo.

Growth factors, such as insulin-like growth factor-I and TGF-α, have been shown to induce the expression of hCAP18/LL-37 and hBD3 in human keratinocytes (49). In addition to these growth factors, EGF family members, including HB-EGF, are known to induce hCAP18/LL-37 in keratinocytes (our unpublished data). The EGF family is thought to be involved in the re-epithelialization of skin wounds (50). Among the EGF family, HB-EGF is a major growth factor component of wound fluid (51). Wound stimuli induce the shedding of HB-EGF from keratinocytes (37). In contrast, the mechanism of induction of hCAP18/LL-37 is poorly understood (4). The induction of hCAP18/LL-37 by EGF family members suggests that the high level of expression of hCAP18/LL-37 on the keratinocytes at the wound edge is due to HB-EGF. In psoriasis, hCAP18/LL-37 is up-regulated in the lesional epidermis (52). Because EGF family expression is enhanced in the lesional skin of psoriasis patients (53, 54), these elevated levels of hCAP18/LL-37 may be due to increased levels of EGF family proteins.

We also analyzed the regulation of STAT3 activation during LL-37-induced keratinocyte migration. The SOCS/CIS family negatively regulates the STAT pathways (34, 55, 56). However, the inhibitory functions of the SOCS/CIS family differ according to the cell type and cellular conditions. In this study, we showed that SOCS1/JAB or SOCS3/CIS3 block LL-37-induced keratinocyte migration, which suggests that migration is inhibited under conditions of high-level SOCS1/JAB or SOCS3/CIS3. Cytokines, such as IFN-γ, IL-4, and IL-6, have been implicated in a variety of physiological and pathological conditions of the skin. IFN-γ enhances SOCS1/JAB and SOCS3/CIS3 expression (41) in normal human keratinocytes. In addition, IL-4 and IL-6 enhance the expression of SOCS1/JAB and SOCS3/CIS3, respectively, in normal human keratinocytes (41). Therefore, the possibility exists that IFN-γ, IL-4, and IL-6 affect wound healing in various inflammatory skin conditions by regulating keratinocyte migration via the induction of SOCS1/JAB or SOCS3/CIS3, which would lead to sustained wound healing in chronic ulcers. However, SOCS1/JAB and SOCS3/CIS3 were not induced by LL-37, which indicates that SOCS1/JAB and SOCS3/CIS3 do not act as self-limiting factors in LL-37-induced keratinocyte migration.

In conclusion, LL-37 induces keratinocyte migration via HB-EGF-mediated EGFR transactivation and STAT3 phosphorylation.

Acknowledgments

We thank Teruko Tsuda and Eriko Tan for significant technical assistance.

Disclosures

The authors have no financial conflict of interest.

References

1. Ganz, T. 2003. Defensins: antimicrobial peptides of innate immunity. *Nat. Rev. Immunol.* 3: 710–720.
2. Lehrer, R. I., and T. Ganz. 1999. Antimicrobial peptides in mammalian and insect host defence. *Curr. Opin. Immunol.* 11: 23–27.
3. Yang, D., O. Chertov, and J. J. Oppenheim. 2001. Participation of mammalian defensins and cathelicidins in anti-microbial immunity: receptors and activities of human defensins and cathelicidin (LL-37). *J. Leukocyte Biol.* 69: 691–697.
4. Zaiou, M., and R. L. Gallo. 2002. Cathelicidins, essential gene-encoded mammalian antibiotics. *J. Mol. Med.* 80: 549–561.
5. Ganz, T., M. E. Selsted, D. Szklarek, S. S. Harwig, K. Daher, D. F. Bainton, and R. I. Lehrer. 1985. Defensins: natural peptide antibiotics of human neutrophils. *J. Clin. Invest.* 76: 1427–1435.
6. Selsted, M. E., S. S. Harwig, T. Ganz, J. W. Schilling, and R. I. Lehrer. 1985. Primary structures of three human neutrophil defensins. *J. Clin. Invest.* 76: 1436–1439.
7. Jones, D. E., and C. L. Bevins. 1993. Defensin-6 mRNA in human paneth cells: implications for antimicrobial peptides in host defense of the human bowel. *FEBS Lett.* 315: 187–192.
8. Quayle, A. J., E. M. Porter, A. A. Nussbaum, Y. M. Wang, C. Brabec, K. P. Yip, and S. C. Mok. 1998. Gene expression, immunolocalization, and secretion of human defensin-5 in human female reproductive tract. *Am. J. Pathol.* 152: 1247–1258.
9. Harder, J., J. Bartels, E. Christophers, and J. M. Schroder. 2001. Isolation and characterization of human β-defensin-3, a novel human inducible peptide antibiotic. *J. Biol. Chem.* 276: 5707–5713.
10. Harder, J., J. Bartels, E. Christophers, and J.-M. Schroder. 1997. A peptide antibiotic from human skin. *Nature* 387: 861.
11. Valore, E. V., C. H. Park, A. J. Quayle, K. R. Wiles, P. B. McCray, Jr., and T. Ganz. 1998. Human β-defensin-1: an antimicrobial peptide of urogenital tissues. *J. Clin. Invest.* 101: 1633–1642.
12. Harder, J., U. Meyer-Hoffert, K. Wehkamp, L. Schwichtenberg, and J. M. Schroder. 2004. Differential gene induction of human β-defensins (hBD-1, -2, -3, and -4) in keratinocytes is inhibited by retinoic acid. *J. Invest. Dermatol.* 123: 522–529.
13. Sorensen, O. E., P. Follin, A. H. Johnsen, J. Calafat, G. S. Tjabringa, P. S. Hiemstra, and N. Borregaard. 2001. Human cathelicidin, hCAP-18, is processed to the antimicrobial peptide LL-37 by extracellular cleavage with proteinase 3. *Blood* 97: 3951–3959.
14. Murakami, M., T. Ohtake, R. A. Dorschner, B. Schittek, C. Garbe, and R. L. Gallo. 2002. Cathelicidin anti-microbial peptide expression in sweat, an innate defense system for the skin. *J. Invest. Dermatol.* 119: 1090–1095.
15. Di Nardo, A., A. Vitiello, and R. L. Gallo. 2003. Cutting edge: mast cell antimicrobial activity is mediated by expression of cathelicidin antimicrobial peptide. *J. Immunol.* 170: 2274–2278.
16. Nizet, V., T. Ohtake, X. Lauth, J. Trowbridge, J. Rudisill, R. A. Dorschner, V. Pestonjamasp, J. Piraino, K. Huttner, and R. L. Gallo. 2001. Innate antimicrobial peptide protects the skin from invasive bacterial infection. *Nature* 414: 454–457.
17. Frohm, M., H. Gunne, A. C. Bergman, B. Agerberth, T. Bergman, A. Boman, S. Liden, H. Jornvall, and H. G. Boman. 1996. Biochemical and antibacterial analysis of human wound and blister fluid. *Eur. J. Biochem.* 237: 86–92.
18. Dorschner, R. A., V. K. Pestonjamasp, S. Tamakuwala, T. Ohtake, J. Rudisill, V. Nizet, B. Agerberth, G. H. Gudmundsson, and R. L. Gallo. 2001. Cutaneous injury induces the release of cathelicidin anti-microbial peptides active against group A *Streptococcus*. *J. Invest. Dermatol.* 117: 91–97.
19. Heilborn, J. D., M. F. Nilsson, G. Kratz, G. Weber, O. Sorensen, N. Borregaard, and M. Stahle-Backdahl. 2003. The cathelicidin anti-microbial peptide LL-37 is involved in re-epithelialization of human skin wounds and is lacking in chronic ulcer epithelium. *J. Invest. Dermatol.* 120: 379–389.
20. Elsbach, P. 2003. What is the real role of antimicrobial polypeptides that can mediate several other inflammatory responses? *J. Clin. Invest.* 111: 1643–1645.
21. Yang, D., O. Chertov, S. N. Bykovskaia, Q. Chen, M. J. Buffo, J. Shogan, M. Anderson, J. M. Schroder, J. M. Wang, O. M. Howard, and J. J. Oppenheim. 1999. β-Defensins: linking innate and adaptive immunity through dendritic and T cell CCR6. *Science* 286: 525–528.
22. De, Y., Q. Chen, A. P. Schmidt, G. M. Anderson, J. M. Wang, J. Wooters, J. J. Oppenheim, and O. Chertov. 2000. LL-37, the neutrophil granule- and epithelial cell-derived cathelicidin, utilizes formyl peptide receptor-like 1 (FPRL1) as a receptor to chemoattract human peripheral blood neutrophils, monocytes, and T cells. *J. Exp. Med.* 192: 1069–1074.
23. Davidson, D. J., A. J. Currie, G. S. Reid, D. M. Bowdish, K. L. MacDonald, R. C. Ma, R. E. Hancock, and D. P. Speert. 2004. The cationic antimicrobial peptide LL-37 modulates dendritic cell differentiation and dendritic cell-induced T cell polarization. *J. Immunol.* 172: 1146–1156.
24. Koczulla, R., G. von Degenfeld, C. Kupatt, F. Krotz, S. Zahler, T. Gloe, K. Issbrucker, P. Unterberger, M. Zaiou, C. Lebherz, et al. 2003. An angiogenic role for the human peptide antibiotic LL-37/hCAP-18. *J. Clin. Invest.* 111: 1665–1672.
25. Sarret, Y., D. T. Woodley, K. Grigsby, K. Wynn, and E. J. O'Keefe. 1992. Human keratinocyte locomotion: the effect of selected cytokines. *J. Invest. Dermatol.* 98: 12–16.

26. McCawley, L. J., P. O'Brien, and L. G. Hudson. 1997. Overexpression of the epidermal growth factor receptor contributes to enhanced ligand-mediated motility in keratinocyte cell lines. *Endocrinology* 138: 121–127.
27. Daub, H., F. U. Weiss, C. Wallasch, and A. Ullrich. 1996. Role of transactivation of the EGF receptor in signalling by G-protein-coupled receptors. *Nature* 379: 557–560.
28. Miyamoto, S., H. Teramoto, J. S. Gutkind, and K. M. Yamada. 1996. Integrins can collaborate with growth factors for phosphorylation of receptor tyrosine kinases and MAP kinase activation: roles of integrin aggregation and occupancy of receptors. *J. Cell Biol.* 135: 1633–1642.
29. Prenzel, N., E. Zwick, H. Daub, M. Leserer, R. Abraham, C. Wallasch, and A. Ullrich. 1999. EGF receptor transactivation by G-protein-coupled receptors requires metalloproteinase cleavage of proHB-EGF. *Nature* 402: 884–888.
30. Asakura, M., M. Kitakaze, S. Takashima, Y. Liao, F. Ishikura, T. Yoshinaka, H. Ohmoto, K. Node, K. Yoshino, H. Ishiguro, et al. 2002. Cardiac hypertrophy is inhibited by antagonism of ADAM12 processing of HB-EGF: metalloproteinase inhibitors as a new therapy. *Nat. Med.* 8: 35–40.
31. Tjabringa, G. S., J. Aarbiou, D. K. Ninaber, J. W. Drijfhout, O. E. Sorensen, N. Borregaard, K. F. Rabe, and P. S. Hiemstra. 2003. The antimicrobial peptide LL-37 activates innate immunity at the airway epithelial surface by transactivation of the epidermal growth factor receptor. *J. Immunol.* 171: 6690–6696.
32. Sano, S., S. Itami, K. Takeda, M. Tarutani, Y. Yamaguchi, H. Miura, K. Yoshikawa, S. Akira, and J. Takeda. 1999. Keratinocyte-specific ablation of Stat3 exhibits impaired skin remodeling, but does not affect skin morphogenesis. *EMBO J.* 18: 4657–4668.
33. Leonard, W. J., and J. J. O'Shea. 1998. Jaks and STATs: biological implications. *Annu. Rev. Immunol.* 16: 293–322.
34. Duhe, R. J., L. H. Wang, and W. L. Farrar. 2001. Negative regulation of Janus kinases. *Cell Biochem. Biophys.* 34: 17–59.
35. Tokumaru, S., K. Sayama, K. Yamasaki, Y. Shirakata, Y. Hanakawa, Y. Yahata, X. Dai, M. Tohyama, L. Yang, A. Yoshimura, and K. Hashimoto. 2005. SOCS3/CIS3 negative regulation of STAT3 in HGF-induced keratinocyte migration. *Biochem. Biophys. Res. Commun.* 327: 100–105.
36. Midorikawa, K., K. Ouhara, H. Komatsuzawa, T. Kawai, S. Yamada, T. Fujiwara, K. Yamazaki, K. Sayama, M. A. Taubman, H. Kurihara, et al. 2003. *Staphylococcus aureus* susceptibility to innate antimicrobial peptides, β-defensins and CAP18, expressed by human keratinocytes. *Infect. Immun.* 71: 3730–3739.
37. Tokumaru, S., S. Higashiyama, T. Endo, T. Nakagawa, J. I. Miyagawa, K. Yamamori, Y. Hanakawa, H. Ohmoto, K. Yoshino, Y. Shirakata, et al. 2000. Ectodomain shedding of epidermal growth factor receptor ligands is required for keratinocyte migration in cutaneous wound healing. *J. Cell Biol.* 151: 209–220.
38. Sayama, K., Y. Shirakata, K. Midorikawa, Y. Hanakawa, and K. Hashimoto. 1999. Possible involvement of p21 but not of p16 or p53 in keratinocyte senescence. *J. Cell Physiol.* 179: 40–44.
39. Shirakata, Y., H. Ueno, Y. Hanakawa, K. Kameda, K. Yamasaki, S. Tokumaru, Y. Yahata, M. Tohyama, K. Sayama, and K. Hashimoto. 2004. TGF-β is not involved in early phase growth inhibition of keratinocytes by 1α,25(OH)2vitamin D3. *J. Dermatol. Sci.* 36: 41–50.
40. Boyden, S. 1962. The chemotactic effect of mixtures of antibody and antigen on polymorphonuclear leucocytes. *J. Exp. Med.* 115: 453–466.
41. Yamasaki, K., Y. Hanakawa, S. Tokumaru, Y. Shirakata, K. Sayama, T. Hanada, A. Yoshimura, and K. Hashimoto. 2003. Suppressor of cytokine signaling 1/JAB and suppressor of cytokine signaling 3/cytokine-inducible SH2 containing protein 3 negatively regulate the signal transducers and activators of transcription signaling pathway in normal human epidermal keratinocytes. *J. Invest. Dermatol.* 120: 571–580.
42. Miyake, S., M. Makimura, Y. Kanegae, S. Harada, Y. Sato, K. Takamori, C. Tokuda, and I. Saito. 1996. Efficient generation of recombinant adenoviruses using adenovirus DNA-terminal protein complex and a cosmid bearing the full-length virus genome. *Proc. Natl. Acad. Sci. USA* 93: 1320–1324.
43. Elssner, A., M. Duncan, M. Gavrilin, and M. D. Wewers. 2004. A novel P2X7 receptor activator, the human cathelicidin-derived peptide LL37, induces IL-1β processing and release. *J. Immunol.* 172: 4987–4994.
44. Braff, M. H., M. A. Hawkins, A. Di Nardo, B. Lopez-Garcia, M. D. Howell, C. Wong, K. Lin, J. E. Streib, R. Dorschner, D. Y. Leung, and R. L. Gallo. 2005. Structure-function relationships among human cathelicidin peptides: dissociation of antimicrobial properties from host immunostimulatory activities. *J. Immunol.* 174: 4271–4278.
45. Frohm, M., B. Agerberth, G. Ahangari, M. Stahle-Backdahl, S. Liden, H. Wigzell, and G. H. Gudmundsson. 1997. The expression of the gene coding for the antibacterial peptide LL-37 is induced in human keratinocytes during inflammatory disorders. *J. Biol. Chem.* 272: 15258–15263.
46. Johansson, J., G. H. Gudmundsson, M. E. Rottenberg, K. D. Berndt, and B. Agerberth. 1998. Conformation-dependent antibacterial activity of the naturally occurring human peptide LL-37. *J. Biol. Chem.* 273: 3718–3724.
47. Inoue, M., G. Kratz, A. Haegerstrand, and M. Stahle-Backdahl. 1995. Collagenase expression is rapidly induced in wound-edge keratinocytes after acute injury in human skin, persists during healing, and stops at re-epithelialization. *J. Invest. Dermatol.* 104: 479–483.
48. Kratz, G. 1998. Modeling of wound healing processes in human skin using tissue culture. *Microsc. Res. Tech.* 42: 345–350.
49. Sorensen, O. E., J. B. Cowland, K. Theilgaard-Monch, L. Liu, T. Ganz, and N. Borregaard. 2003. Wound healing and expression of antimicrobial peptides/polypeptides in human keratinocytes, a consequence of common growth factors. *J. Immunol.* 170: 5583–5589.
50. Martin, P. 1997. Wound healing–aiming for perfect skin regeneration. *Science* 276: 75–81.
51. Marikovsky, M., K. Breuing, P. Y. Liu, E. Eriksson, S. Higashiyama, P. Farber, J. Abraham, and M. Klagsbrun. 1993. Appearance of heparin-binding EGF-like growth factor in wound fluid as a response to injury. *Proc. Natl. Acad. Sci. USA* 90: 3889–3893.
52. Ong, P. Y., T. Ohtake, C. Brandt, I. Strickland, M. Boguniewicz, T. Ganz, R. L. Gallo, and D. Y. Leung. 2002. Endogenous antimicrobial peptides and skin infections in atopic dermatitis. *N. Engl. J. Med.* 347: 1151–1160.
53. Elder, J. T., G. J. Fisher, P. B. Lindquist, G. L. Bennett, M. R. Pittelkow, R. J. Coffey, Jr., L. Ellingsworth, R. Derynck, and J. J. Voorhees. 1989. Overexpression of transforming growth factor α in psoriatic epidermis. *Science* 243: 811–814.
54. Cook, P. W., M. R. Pittelkow, W. W. Keeble, R. Graves-Deal, R. J. Coffey, Jr., and G. D. Shipley. 1992. Amphiregulin messenger RNA is elevated in psoriatic epidermis and gastrointestinal carcinomas. *Cancer Res.* 52: 3224–3227.
55. Naka, T., M. Narazaki, M. Hirata, T. Matsumoto, S. Minamoto, A. Aono, N. Nishimoto, T. Kajita, T. Taga, K. Yoshizaki, et al. 1997. Structure and function of a new STAT-induced STAT inhibitor. *Nature* 387: 924–929.
56. Alexander, W. S., R. Starr, J. E. Fenner, C. L. Scott, E. Handman, N. S. Sprigg, J. E. Corbin, A. L. Cornish, R. Darwiche, C. M. Owczarek, et al. 1999. SOCS1 is a critical inhibitor of interferon γ signaling and prevents the potentially fatal neonatal actions of this cytokine. *Cell* 98: 597–608.

The Journal of Dermatology
Vol. 32: 278–281, 2005

Drug-Induced Hypersensitivity Syndrome due to Mexiletine Associated with Human Herpes Virus 6 and Cytomegalovirus Reactivation

Atsushi Sekiguchi, Takayuki Kashiwagi, Akemi Ishida-Yamamoto, Hidetoshi Takahashi, Yoshio Hashimoto, Hiroshi Kimura*, Mikiko Tohyama**, Koji Hashimoto** and Hajime Iizuka

Abstract

A 66-year-old man developed a fever of 38°C and generalized pruritic rash about one month after mexiletine hydrochloride administration for ventricular tachycardia. The rash appeared as edematous erythema and papules with purpura on the lower extremities. Liver dysfunction, leukocytosis, and atypical lymphocytes were also present. Elevated antibody titer against human herpes virus 6 (HHV-6) was detected during the course of the disease (1:20 -> 1:640). The patient was diagnosed as having drug-induced hypersensitivity syndrome (DIHS) due to mexiletine. Discontinuation of the mexiletine administration and systemic corticosteroid treatment led to a temporary improvement, but tapering the corticosteroid dose twice led to recrudescence. Simultaneous with the recrudescence, elevated antibody titers against HHV-6 and cytomegalovirus were detected, as well as viral DNA in the blood, suggesting that these two viruses may have been involved in the recrudescence. The patient died of myocarditis, most likely related to cytomegalovirus. Our case indicates that, in addition to HHV-6, other herpes viruses such as cytomegalovirus can be reactivated in DIHS and may modify the clinical disease activity.

Key words: drug-induced hypersensitivity syndrome; human herpes virus 6 (HHV-6); cytomagalovirus

Introduction

Drug-induced hypersensitivity syndrome (DIHS) is a severe form of drug reaction characterized by high fever, facial edema, maculopapular rash and/or erythroderma, generalized lymphadenopathy, hypereosinophilia, atypical circulating lymphocytes, and abnormal liver function tests (1–6). Notably, the drugs that induce DIHS are relatively restricted; these include anticonvulsants, salazosulfapyridine, allopurinol, minocycline, and mexiletine. It has been reported that human herpes virus type 6 (HHV-6) participates in the pathogenesis of DIHS. However, reactivation of viruses other than HHV-6 has also been implicated, suggesting a complex interaction between drugs and viruses in the pathogenesis of this disease entity. Herein, we report a patient with DIHS due to mexiletine hydrochloride, in whom reactivation of both HHV-6 and cytomegalovirus (CMV) was detected.

Received June 25, 2004; accepted for publication November 2, 2004.

Department of Dermatology, Asahikawa Medical College, Asahikawa, Japan.
*Department of Pediatrics/Developmental Pediatrics, Nagoya University Graduate School of Medicine, Nagoya, Japan.
**Department of Dermatology, Ehime University, School of Medicine, Tou-on, Japan.
Reprint requests to: Hajime Iizuka, M.D., Department of Dermatology, Asahikawa Medical College, Midorigaoka-Higashi 2-1-1-1, Asahikawa 078-8510, Japan.

Case Report

A 66 year-old male with a history of acute myocardial infarction and ventricular tachycardia was started on mexiletine hydrochloride on December 15, 2001. Fever of 38–39°C and generalized pruritic rash developed from January 11,

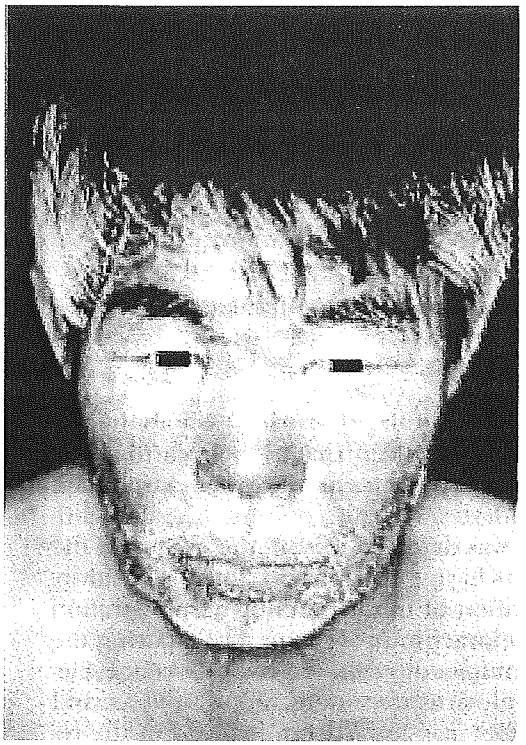

Fig. 1. Edematous erythema on the face of the patient. Similar edematous erythema was seen on almost the entire body.

2002. The symptoms worsened gradually, and the patient was admitted for evaluation. On admission, infiltrative erythematous papules and light red edematous erythema were found scattered over the body and all extremities (Fig. 1). In some areas, the lesions had coalesced to form irregular plaques. Miliary-sized to fingertip-sized purpuric lesions were seen within the erythematous areas in the lower thigh and dorsum of the foot. Erythema with an ill-defined border was seen on the face. There was no enanthema, lymphadenopathy, or hepatosplenomegaly. Laboratory findings were as follows: WBC count 9,800/mm^3 (44% neut, 13% eos, 2% mono, 37% lymph), RBC count 444 × 10^4/mm^3, Hb 14.4 g/dL, Plt 20.7 × 10^4/mm^3, TP 6.8 g/dL, AST 51 IU/L, ALT 48 IU/L, LDH 742 IU/L, γGTP 160 IU/L BUN 15.5 mg/dL, creatinine 1.1 mg/dL, CRP 1.1 mg/dL , IgE 322 U/mL. Histopathological findings disclosed a slightly acanthotic epidermis and perivascular cellular infiltration composed mostly of lymphocytes and eosinophils. Extravasation of erythrocytes was also seen.

Based on the drug history, characteristic generalized rash, and the laboratory findings, DIHS was suspected, and mexiletine hydrochloride was stopped. The patient was treated with oral prednisolone at 40 mg/day. Initially, the fever in the upper 37°C range continued with no resolution of the systemic rash. On day 10 after the onset of illness, atypical lymphocytes were observed. On day 17, the patient developed leukocytosis with a WBC count of 41,200/mm^3 and liver dysfunction with AST 245 IU/L and ALT 561 IU/L. On day 18 after the onset of illness, the fever and rash improved with an improvement in the liver function.

On day 21, the prednisolone was tapered to 30 mg. On day 24 after the onset of illness, however, the patient experienced a recurrence of fevers in the 38–39°C range and worsening of the rash in the extremities, but these findings improved by day 26. On day 33 after the onset of illness, prednisolone was tapered to 20 mg. On day 38, the patient again experienced a recurrence of systemic erythema and fevers in the 38–39°C range. On the following day, the patient had systemic deterioration with hypotension. Medical evaluation identified myocarditis, and, despite the treatment, he died on March 3, 2002, from heart failure. Autopsy was not performed.

HHV-6 titer measured by an immunofluorescent method was negative for both IgG and IgM on day 12 after onset of illness, but the anti-HHV-6 IgG titer rapidly rose to 1:20 on day 27, 1:160 on day 32, and 1:640 on day 38 (Table 1). HHV-6 DNA was also detected in the blood by PCR. During this period the patient also showed an increase in the CMV IgG titer as detected by ELISA (6.7 to 16), and the CMV DNA in the blood also became detectable on day 27 and continued to increase to day 38 (Table 1).

Discussion

DIHS is a severe form of drug eruption in which HHV-6 reactivation is considered to be involved; it is characterized by fever and lymphadenopathy with organ injury such as hepatic and renal dysfunction (1–6). In our

Table 1. Laboratory data

	Days after onset of skin eruption									
	0	6	10	12	17	20	24	27	32	38
WBC (/mm3)		9,800	18,200	28,700	41,200	23,700	11,300	7,100	8,400	7,100
Aty-lym (%)		0	1	0	0	0	1	0	0	0
Eo (%)		13	11	22	33	19	23	4	2	8
AST (IU/l)		51	142	203	245	134	198	183	68	67
ALT (IU/l)		48	231	314	561	429	549	505	304	196
BUN (IU/l)		15	37	39	26	25	29	29	31	23
Cre (IU/l)		1.1	2.3	1.4	1.0	0.9	1.4	1.5	1.3	1.3
HHV-6										
IgG				<20			<20	20	160	640
IgM				<10			<10	<10	—	20
DNA (copy/μgDNA)				—			1,300	25,000	500	190
CMV										
IgG				6.7			12	12	13	16
IgM				<1.2			<1.2	<1.2	<1.2	<1.2
DNA (copy/μgDNA)				—			0	9,000	26,000	31,000

WBC: white blood cell, Aty-lym: atypical lymphocyte, Eo: Eosinophil, AST: L-aspartate: 2-oxoglutarate aminotransferase, ALT: L-alanine: 2-oxoglutarate aminotransfarase, BUN: blood urea nitrogen, Cre: creatinine, HHV: human herpesvirus, CMV: cytomegalovirus

case, one month after the initiation of mexiletine hydrochloride, the patient developed fever associated with generalized edematous erythema, leukocytosis, and liver function abnormalities, leading to the diagnosis of DIHS. Elevations of HHV-6 antibody titer and HHV-6 viral DNA were detected during the clinical course.

Recent reports have noted that patients with DIHS have elevations of antibody titers against viruses other than HHV-6. Arakawa et al.(7) reported a patient in whom allopurinol-induced DIHS was associated with HHV-6 reactivation and an elevation of CMV antibody titer, while Aihara et al.(8) reported a patient with DIHS with a reactivation only of CMV. In addition, cases of DIHS associated with elevated serum antibody titers against HHV-7, EB virus, parvovirus B19, rubella virus, and VZV, have also been reported (1, 9, 10).

HHV-6 IgG and HHV-6 DNA were detected in our patient, as well as elevated CMV IgG and CMV DNA in the blood. Approximately 80–90% of the adult Japanese population has been infected with CMV. Most have asymptomatic infections, but CMV reactivation in immunocompromised hosts can result in interstitial pneumonia, myocarditis, enteritis, hepatitis, cholangitis, retinitis, and encephalitis (11–13). Our patient is unique in that both HHV-6 DNA and CMV DNA were detected during the course of the disease.

In DIHS, the elevation of virus antibody titer occurs 2–3 weeks after the onset of illness and often coincides with recrudescence of symptoms. Based on this observation, Tohyama et al. suggested that the pathogenesis of DIHS involves the reactivation of HHV-6 following the drug allergy (2). Our patient experienced the first recrudescence on day 24 of illness and the second recrudescence on day 38; these dates coincide with the peaks of HHV-6 DNA and CMV-DNA levels seen on day 27 and day 38. With respect to the serum antibody titer, HHV-6 IgG antibody titer began to rise on day 27, while the

CMV IgG titer began to rise on day 24. The rise in CMV antibody titer was less than 4-fold (ELISA 6.7 -> 16); however, it was associated with increased viral DNA copy number in the blood (Table 1). As seen in our patient, the findings of a coincidental increase of the virus and the recrudescence of clinical manifestations strongly suggest the involvement of viral reactivation in the pathogenesis of DIHS. Although HHV-6 IgG antibody titer was initially negative, a finding which might suggest primary infection, the pattern of changes in the IgM antibody titer was not consistent.

Our patient developed myocarditis during the second recrudescence. CMV is known to cause myocarditis (11), and it is conceivable that the DIHS-associated CMV reactivation may have been the direct cause of death, although no autopsy could not be performed to confirm this. DIHS is a severe type of drug eruption in which the involvement of HHV-6 is strongly suspected, but as in our patient, the involvement of other herpes viruses such as CMV and HHV-7 (1) has also been reported. Because CMV can affect systemic organ function and effective treatments such as ganciclovir and CMV high titer gamma globulin preparations are available (14), patients with DIHS, which is usually treated with systemic corticosteroid administration (15), must be carefully evaluated for viruses other than HHV-6.

References

1) Suzuki Y, Inagi R, Aono T, Yamanishi K, Shiohara T: Human herpesvirus 6 infection as a risk factor for the development of severe drug-induced hypersensitivity syndrome, *Arch Dermatol*, **134**: 1108–1112, 1998.
2) Tohyama M, Yahata Y, Yasukawa M, et al: Severe hypersensitivity syndrome due to sulfasalazine associated with reactivation of human herpesvirus 6, *Arch Dermatol*, **134**: 1113–1137, 1998.
3) Descamps V, Valance A, Edlinger C, et al: Association of human herpes virus 6 infection with drug reaction with eosinophilia and systemic symptoms, *Arch Dermatol*, **137**: 301–304, 2001.
4) Sullivan JR, Shear NH: The drug hypersensitivity syndrome: what is the pathogenesis ?, *Arch Dermatol*, **137**: 357–364, 2001.
5) Descamps V, Collot S, Mahe E, Houhou N, Crickx B, Ranger-Rogez S: Active human herpes virus 6 infection in a patient with drug rash with eosinophilia and systemic symptoms, *J Invest Dermatol*, **121**: 215–216, 2003.
6) Descamps V, Bouscarat F, Laglenne S, et al: Human herpesvirus 6 infection associated with anticonvulsant hypersensitivity syndrome and reactive haemophagocytic syndrome, *Br J Dermatol*, **137**: 605–608, 1997.
7) Arakawa M, Kakuto Y, Ichikawa K, Chiba J, Tabata N, Sasaki Y: Allopurinol hypersensitivity syndrome associated with systemic cytomegalovirus infection and systemic bacteremia, *Int Med*, **40**: 331–335, 2001.
8) Aihara M, Sugita Y, Takahashi S, et al: Anticonvulsant hypersensitivity syndrome associated with reactivation of cytomegalovirus, *Br J Dermatol*, **144**: 1232–1234, 2001.
9) Regnier S, Descamps V, Boui M, et al: Parvovirus B19 infection mimicking drug-induced hypersensitivity syndrome [French], *Annales de Dermatologie Venereologie*, **127**: 505–506, 2000.
10) Descamps V, Mahe E, Houhou N, et al: Drug-induced hypersensitivity syndrome associated with Epstein-Barr virus infection, *Br J Dermatol*, **148**: 1032–1034, 2003.
11) Pankuweit S, Portig I, Eckhardt H, Crombach M, Hufnagel G, Maisch B: Prevalence of viral genome in endomyocardial biopsies from patients with inflammatory heart muscle disease, *Herz*, **25**: 221–226, 2000.
12) de la Hoz RE, Stephens G, Sherlock C: Diagnosis and treatment approaches of CMV infections in adult patients, *J Clin Virol*, **25** (Suppl 2): s1–s12, 2002.
13) Baumal CR, Levin AV, Read SE: Cytomegalovirus retinitis in immunosuppressed children, *Am J Ophthalmol*, **127**: 550–558, 1999.
14) Glowacki LS, Smaill FM: Use of immune globulin to prevent symptomatic cytomegalovirus disease in transplant recipients—A meta-analysis, *Clin Transplant*, **8**: 10–18, 1994.
15) Roujeau JC: Treatment of severe drug eruptions, *J Dermatol*, **26**: 718–722, 1999.

Urokinase-induced activation of the gp130/Tyk2/Stat3 pathway mediates a pro-inflammatory effect in human mesangial cells via expression of the anaphylatoxin C5a receptor

Nelli Shushakova[1], Natalia Tkachuk[1], Marc Dangers[1], Sergey Tkachuk[1], Joon-Keun Park[1], Joerg Zwirner[2], Koji Hashimoto[3], Hermann Haller[1] and Inna Dumler[1,4,*]

[1]Hannover Medical School, Carl-Neuberg Straße 1, 30625 Hannover, Germany
[2]Department of Immunology, Georg-August-University, Kreuzbergring 57, 37073 Göttingen, Germany
[3]Ehime University School of Medicine, Shitsukawa, Shigenobucho, Onsengun, Ehime 791-0295, Japan
[4]Medical Faculty of the Charité–Franz Volhard Clinic, HELIOS Klinikum-Berlin and Max Delbrück Center for Molecular Medicine, Wiltbergstrasse 50, 13125 Berlin, Germany
*Author for correspondence (e-mail: dumler.inna@mh-hannover.de)

Accepted 30 March 2005
Journal of Cell Science 118, 2743-2753 Published by The Company of Biologists 2005
doi:10.1242/jcs.02409

Summary

Glomerular mesangial cells (MCs) are central to the pathogenesis of progressive glomeruli-associated renal diseases. However, molecular mechanisms underlying changes in MC functions still remain poorly understood. Here, we show that in MCs, the urokinase-type plasminogen activator (uPA) induces, via its specific receptor (uPAR, CD87), upregulated expression of the complement anaphylatoxin C5a receptor (C5aR, CD88), and modulates C5a-dependent functional responses. This effect is mediated via the interaction of the uPA-specific receptor (uPAR, CD87) and gp130, a signal transducing subunit of the receptor complexes for the IL-6 cytokine family. The Janus kinase Tyk2 and the transcription factor Stat3 serve as downstream components in the signaling cascade resulting in upregulation of C5aR expression. In vivo, expression of C5aR and uPAR was increased in the mesangium of wild-type mice in a lipopolysaccharide (LPS)-induced model of inflammation, whereas in *uPAR*$^{-/-}$ animals C5aR expression remained unchanged. This is the first demonstration in vitro and in vivo that uPA acts in MCs as a modulator of immune responses via control of immune-competent receptors. The data suggest a novel role for uPA/uPAR in glomeruli-associated renal failure via a signaling cross-talk between the fibrinolytic and immune systems.

Key words: Urokinase, uPA receptor, C5a receptor, Mesangial cells, Inflammation

Introduction

The early stages of inflammatory processes are accompanied by activation of the complement system. One of the biological consequences of this activation is the release of potent inflammatory molecules, C3a and C5a anaphylatoxins. Anaphylatoxins act through specific receptors that are members of the rhodopsin family of seven transmembrane-spanning G protein-linked receptors (Gerard and Gerard, 1994). Expression of these receptors, initially thought to be restricted to peripheral blood leukocytes, appears to occur in several tissues. Recent reports provide evidence for the expression of anaphylatoxin C5a receptor (C5aR, CD88) on human mesangial cells (MCs), which play a pivotal role in renal physiology (Braun and Davis III, 1998; Wilmer et al., 1998). Moreover, C5aR activation in MCs induced proliferation, selective production of cytokines and growth factors, as well as upregulation of certain transcription factors and early response genes (Wilmer et al., 1998). All these parameters might determine the degree of mesangial injury, which in turn dictates the final outcome of the inflammatory process. These data indicate a role for the MC-expressed C5aR in mediating glomerular injury and pathogenesis of progressive glomeruli-associated renal diseases. This implication is strengthened by the demonstration of enhanced expression of C5aR in human diseased kidney (Abe et al., 2001) and by the recent studies on C5aR-mediated renal dysfunction (de Vries et al., 2003; Aramugam et al., 2003). However, molecular mechanisms of MC stimulation and upregulated C5aR expression in MCs remain unexplored. Most probably important candidates might be complement proteins, platelet products and components of the fibrinolytic system, in particular the urokinase-type plasminogen activator (uPA) and its specific receptor (uPAR, CD87).

uPA is a multifunctional molecule that serves either as a proteolytic enzyme or as a signal-inducing ligand. The urokinase receptor uPAR was originally identified as a proteinase receptor for uPA, directing pericellular proteolysis. However, uPAR also mediates intracellular signaling via surface proteins such as integrins, growth factors receptors and G-protein-coupled membrane proteins. These dual properties enable the uPA/uPAR system to control pericellular fibrinolytic and proteolytic activities, as well as cell adhesion, migration, proliferation and differentiation (Blasi and Carmeliet, 2002).

Moreover, recent findings in vitro and in vivo indicate that the uPA/uPAR system is an active participant in the majority of infection and inflammatory diseases and might serve as a modulator of immunological responses (Gyetko et al., 1996; Gyetko et al., 2000; May et al., 1998; Mondino and Blasi, 2004). Remarkably, modulating effects of the uPA/uPAR system on immunological responses may involve not only migration of different types of leukocytes to the site of inflammation but also contribute to generating pro- and anti-inflammatory signals, such as TNF-α neo-synthesis of lipopolysaccharide (LPS)-stimulated mononuclear phagocytes in vitro (Sitrin et al., 1996) and IFN-γ and IL-12 in vivo in response to pulmonary infection (Gyetko et al., 2002). Moreover, in the murine model of endotoxemia-induced lung injury, uPA increases LPS-induced activation of neutrophils via activation of a uPAR-directed intracellular signaling pathways including Akt and c-Jun N-terminal kinase, nuclear translocation of NF-κB and enhanced expression of IL-1β, TNF-α and MIP-2 (Abraham et al., 2003). These data suggest the interplay of the uPA/uPAR system and transcription factors that may represent an important cell-specific mechanism that upregulates the inflammatory response and facilitates MC proliferation upon progressive glomerular diseases.

In this study we show that through Tyk2/Stat3 activation, uPAR occupancy by uPA and its association with gp130 protein, a signal transducing subunit of the IL-6 receptor complexes, upregulates expression of anaphylatoxin C5aR on human MCs and modulates C5aR-dependent functional cell responses. These findings identify components of a novel pathway that couples fibrinolytic and immune systems in kidney inflammatory diseases.

Materials and Methods

Materials

Chemicals of high quality commercial grade were purchased from Sigma, Amersham Bioscience Inc., Merck, Serva (Heidelberg, Germany), Carl Roth GmbH (Karlsruhe, Germany) and Bio-Rad Laboratories (Hercules, CA, USA). Chemiluminescent signal enhancer was obtained from Perkin Elmer Life Sciences (Boston, MA, USA). Mounting medium was purchased from Polysciences, Inc. (Warrington, PA, USA). uPA was from Loxo (Dossenheim, Germany).

Antibodies

Anti-human CD88, anti-human gp130 and horseradish peroxidase-conjugated secondary polyclonal antibodies were from Santa Cruz Biotechnology, Inc. (Santa Cruz, CA, USA). Anti-STAT3 and anti-Tyk2 monoclonal antibodies were from Transduction Laboratories (Lexington, KY, USA), anti-phospho-STAT3 (Tyr705) and anti-phospho-Tyk2 (Tyr1054/1055) polyclonal antibodies were from Cell Signaling Technology (Beverly, MA, USA). Monoclonal anti-human uPAR clone R3 antibody was from Monozyme (Copenhagen, Denmark). Alexa Fluor 488-conjugated goat anti-rabbit and Alexa Fluor 488-conjugated donkey anti-goat antibodies were purchased from Molecular Probes, Inc. (Eugene, OR, USA). Normal rabbit IgG and normal mouse IgG were from Upstate Biotechnology, Inc. (Lake Plasid, NY, USA). Monoclonal anti-mouse C5aR antibodies (clone 2/70, rat anti-mouse IgG) were generated as described previously (Werfel et al., 1996).

Cell culture

Normal human mesangial cells were obtained from Clonetics (San Diego, CA, USA). The cells were cultured in MsGM medium (Clonetics) supplemented with 5% fetal bovine serum (Clonetics) and were used in passage 8. For the uPA stimulation experiments, cells were starved for 24 hours in serum-free medium. For inhibition experiments cells were pretreated before uPA stimulation for 1 hour with the appropriate antibody at 5 μg/ml medium.

Cell infection, Tyk2 and Stat3 expression

Adenoviral Tyk2 constructs were generated as previously described (Kusch et al., 2000). Additionally, the deletion mutant Ad5Tyk2ΔC was generated by removing the kinase domain after amino acid 776. As a control, an adenovirus expressing β-galactosidase (Ad5βGal) was used. Adenoviral Stat3F construct with a point mutation in the tyrosine phosphorylation site at residue 705 (Tyr to Phe) was generated as previously described (Yahata et al., 2003). Cells were grown up to 80% confluency and infected for 1 hour with recombinant adenovirus stock at a multiplicity of infection of 500 plaque-forming units/cell in a total volume of 1 ml/well in six-well plates. The efficiency of infection was assessed by western blotting using anti-Tyk2 or anti-Stat3 antibody, respectively. Cells were serum-starved overnight after 24 hours of infection and used for experiments on the second day after infection. Total RNA was prepared using an RNeasy Kit (QIAGEN GmbH, Germany).

Design and cloning of lentiviral siRNA vectors

The human *uPAR* cDNA sequence (NM 002659) was searched for suitable siRNA target sequences starting with aag followed by 18 nucleotides. The 21 nucleotides sense and antisense sequences were subjected to BLAST searches, eliminating sequences with more than 16 bp homologies in the human genome. uPAR siRNA oligonucleotides (uPARsi): sense, 5′-GATCCCC**AAGCTGTACCCACTCAGAG**TTCAAGAGA**CTCTGAGTGGGTACAGCTT**TTTTTGGAAA; antisense, 5′-AGCTTTTCCAAAAA**AAGCTGTACCCACTCAGAG**TCTCTTGAA**CTCTGAGTGGGTACAGCTT**GGG. Sense and antisense siRNA sequences are shown in bold and loop sequences are underlined. Hybridized oligonucleotides were ligated into the pSuper.retro vector (purchased from Oligo Engine, Seattle, WA, USA), into the *Bgl*II-*Hin*dIII-site, downstream of the H1 promoter. The H1-hairpin-precursor cassette was excised from pSuper.retro with *Eco*RI and *Cla*I (Fermentas GmbH, Germany) and further cloned into *Eco*RI-*Cla*I site of the pLV-TH plasmid.

Lentiviral vector production and cell infection

Lentiviral vectors were produced by transient transfection of 293T cells according to standard protocols. Briefly, 293T cells were cultured in Dulbecco's modified Eagle's medium (DMEM), supplemented with 10% fetal calf serum (FCS) and, when subconfluent, transfected with 15 μg of pCMV-ΔR8.91, 6 μg of pMD2G and 20 μg of pLV-TH-uPARsi, or pLV-TH as control. The transfection was performed by calcium-phosphate precipitation. Medium was changed to DMEM, supplemented with 2% FCS, after 6 to 8 hours. Vector supernatants, containing viral particles, were harvested approximately 48 hours later and concentrated by ultracentrifugation (1.5 hours at 25,000 *g* at 4°C). The virus obtained was assigned as LV-uPARsi. The viral batches were titered on 293 cells. MCs were infected in the presence of 8 μg/ml polybrene with viruses at 10^8 TU/ml and used for experiments day 3 after infection. 95% of cells have been shown to be infected under these conditions.

Quantitative RT-PCR analysis of C5aR in human MCs

The total RNA was isolated from human MCs and real-time quantitative RT-PCR for C5aR was performed on a TaqMan ABI 7700 Sequence Detection System (Applied Biosystems, Foster City, CA,

USA). *GAPDH* was used as a reference gene. The following oligonucleotide primers and probes were used: GAPDH, 5′-GAAGGTGAAGGTCGGAGTC-3′ (sense), 5′-GAAGATGGTGATGGGATTC-3′ (antisense), 6-FAM-CAAGCTTCCCGTTCTCAGCC-TAMRA (probe); C5aR, 5′-GTGGTCCGGGAGGAGTACTTT-3′ (sense), 5′-GCCGTTTGTCGTGGCTGTA-3′ (antisense), 6-FAM-CACCAAAGGTGTTGTGTGGCGTGG-TAMRA (probe).

Immunoprecipitation and western blotting

Subconfluent, serum-starved MCs were treated with 10 nM uPA for 5-30 minutes at 37°C, lysed in RIPA buffer containing 1 mM Na_3VO_4, 1 mM NaF, 1 mM PMSF, 10 μg/ml aprotinin, 10 μg/ml leupeptin. The cell lysates were clarified by centrifugation and 1.3-1.7 mg of total protein was incubated overnight at 4°C with appropriate antibodies and protein A/G PLUS-agarose. The immunoprecipitates were subjected to 7.5% SDS-PAGE, and proteins were transferred to PVDF western blotting membrane (Roche Diagnostics GmbH, Mannheim, Germany). Membranes were probed with appropriate antibodies followed by incubation with horseradish peroxidase-conjugated secondary antibodies. The immune complexes were visualized by an enhanced chemiluminescence detection system.

FACS analysis

MCs unstimulated or stimulated with 20 nM uPA for 20 hours were detached from culture plates with 10 mM EDTA, washed with ice-cold PBS, and stained with a murine monoclonal FITC-conjugated anti-C5a receptor antibody that recognized the extracellular peptide corresponding to residues 1-31 (clone W17/1; Serotec Ltd, Oxford, UK), or a FITC-conjugated isotype matched control antibody (Serotec Ltd, Oxford, UK). FACS analysis was performed with a FACScan instrument (Becton-Dickinson).

Immunofluorescence microscopy

Phospho-Stat3 was detected using polyclonal anti-phospho-Stat3 (Tyr705) antibody (Cell Signaling Technology (Beverly, MA, dilution 1:1000) and Alexa Fluor 488-conjugated goat anti-rabbit antibody (Molecular Probes, Inc., dilution 1:150). For C5aR immunofluorescent staining, cells were incubated for 2 hours at room temperature with polyclonal anti-human C5aR antibody (Santa Cruz Biotechnology, dilution 1:40) and Alexa Fluor 488-conjugated donkey anti-goat secondary antibody (Molecular Probes, Inc., dilution 1:150). Confocal microscopy studies were performed as previously described (Dumler et al., 1998).

Animals

Male *uPAR*$^{-/-}$ mice on a mixed C57BL/6J (75%) × 129 (25%) background and their wild-type littermate controls were kindly provided by P. Carmeliet and M. Dewerchin (Leuven, Belgium) and were further bred under the same pathogen-free conditions in the animal facility of Hanover Medical School. All mice, weighing 25-30 g, were used at 8-12 weeks of age. Experiments were conducted in accordance to the regulations of the local authorities.

LPS-induced nephritis

Mice were injected intraperitoneally with either 50 μg LPS (2.0 mg/kg; *Escherichia coli* serotype O111:B4; Sigma Chemical Co, St Louis, MO, USA) in 200 μl of saline or with saline vehicle alone. At 8 hours after injection, the mice were killed and immediately perfused for 10 minutes through the left ventricle into the opened vena cava at an approximate rate of 1 ml/minute of cold PBS. Perfusion quality was optically controlled by observing the organ color change. Large perfusion volumes were used to remove contaminating C5aR-expressing leukocytes from the blood vessels. The kidneys were then harvested, sectioned, the medulla was removed and pieces of kidney cortex containing predominantly glomeruli were snap frozen for RT-PCR experiments and immunohistochemical staining.

Quantitative RT-PCR analysis of uPA, uPAR, C5aR and MCP-1 expression in mouse kidney cortex

Total RNA was isolated from kidney cortex using the RNeasy Mini Kit (QIAGEN GmbH, Germany) and real-time quantitative RT-PCR for uPA, uPAR, C5aR, and MCP-1 serving as a marker of LPS-induced inflammation was performed on a TaqMan ABI 7700 Sequence Detection System (Applied Biosystems, Foster City, CA). β-tubulin was used as a reference gene. The following oligonucleotide primers and probes were used: β-tubulin, 5′-CACCATGAGCGGCGTCA-3′ (sense), 5′-TTCGAAGGTCAGCATTAAGCTG-3′ (antisense), 6-FAM-ACCTGCCTCCGTTTCCCGGG-TAMRA (probe); MCP-1, 5′-CCAACTCTCACTGAAGCCAGC-3′ (sense), 5′-CAGGCCCAGAAGCATGACA-3′ (antisense) 6-FAM-CTCTC-TTCCTCCACCACCATGCAGGT-TAMRA (probe); uPA, 5′-CGAT-TCTGGAGGACCGCTTA-3′ (sense), 5′-CCAGCTCACAATCCCA-CTCA-3′ (antisense), 6-FAM-CTGTAACATCGAAGGCCGCCCA-ACT-TAMRA (probe); uPAR, 5′-CCACAGCGAAAAGACCAACA-3′ (sense), 5′-CGGTCTCTGTCAGGCTGATGA-3′ (antisense), 6-FAM-ATGAGTTACCGCATGGGCTCCA-TAMRA (probe); C5aR, 5′-TGTGGGTGACAGCCTTCGA-3′ (sense), 5′-CCGCCAGATTC-AGAAACCAG-3′ (antisense), 6-FAM-CCAGACGGGCCGTCAA-ACGC-TAMRA (probe).

Immunohistochemical studies

The cryosections (6 μm) were fixed with ice-cold acetone and air-dried. Non-specific binding sites were blocked with 10% normal donkey serum (Jackson Immuno Research Lab, West Grove, USA) for 30 minutes. Then sections were incubated with the monoclonal rat anti-mouse C5aR antibody for 1 hour. For fluorescent visualization of bound primary antibodies, sections were further incubated with Cy3-conjugated secondary donkey anti-rat antibody (Jackson Immune Research Lab, West Grove, USA) for 1 hour. Specimens were analyzed using a Zeiss Axioplan-2 imaging microscope with the digital image-processing program AxioVision 3.0 (Zeiss, Jena, Germany). C5aR expression in the glomeruli was evaluated in a blind fashion in arbitrary units (0-5+) based on the staining intensity and positivity of the mesangium using the following criteria: 5+: >90% positive glomeruli with strong immunoreactivity; 4+: >75% positive glomeruli with strong immunoreactivity; 3+: >75% positive glomeruli with weak immunoreactivity; 2+: >25% positive glomeruli with weak immunoreactivity; 1+: >10% positive glomeruli with weak immunoreactivity. Fifteen different cortical areas of each kidney (n=6 for each group) were analyzed.

Statistical analysis

All values are expressed as the mean ± s.e.m. To analyze differences in mean values the two-sided unpaired Student's t-test was used; $P<0.05$ was considered significant, and $P<0.01$ was considered highly significant.

Results

uPA upregulates expression of C5aR in MCs

We began by examining the ability of uPA to regulate expression of C5aR in normal human mesangial cells. The changes in C5aR expression were monitored at the mRNA and protein levels using TaqMan analysis and immunoblotting, respectively. Treatment of MCs with physiological

concentrations of uPA resulted in dramatic increase (up to sevenfold) in C5aR mRNA. This activation was time-dependent and reversible, starting as early as 4 hours, peaking at 16 hours, and returned to basal level at 48 hours (Fig. 1A). Consistent with these data, C5aR protein expression was also upregulated, as shown by immunoblotting using specific anti-C5aR antibody (Fig. 1B). Additionally, we performed FACS analysis and immunocytochemical studies to visualize and quantify C5aR on the cell surface. Indeed, treatment of MCs with uPA led to substantial expression of C5aR on the surface of stimulated cells (Fig. 1C,D). To verify whether uPA exerts its effect on C5aR activation via uPAR, specific uPAR-blocking antibody was used for cell pretreatment. Neither C5aR mRNA nor C5aR protein was upregulated in response to uPA after uPAR blockage (Fig. 2). These data suggest a requirement for uPAR in the chain of signaling events mediating uPA-induced C5aR expression.

uPA potentiates C5aR-related responses in MCs

Since C5aR activation in MCs was shown to induce proliferation and selective production of cytokines and growth factors, we tested whether these functional C5aR-directed responses might be affected by uPA. MCs were stimulated with uPA and C5a separately and simultaneously, and then cell proliferation and production of MCP-1 were analyzed (Fig. 3). In both cases stimuli worked synergistically when added together. These data provide evidence that uPA functions as a modulator of the C5aR-dependent processes in human MCs. To verify the role of uPAR in the observed effects, MCs were pretreated with uPAR blocking antibody. This antibody, in contrast to non-relevant IgG, abolished synergistic effects of uPA and C5a for both MC proliferation and MCP-1 release (Fig. 3).

uPA induces activation of Stat3 and Tyk2 in MCs

Next, we investigated the molecular mechanisms underlying the revealed uPA-induced expression of C5aR. As no data on signaling pathways mediating C5aR expression are available, we asked whether the signal transducer and activator of transcription Stat3 might be one likely candidate. This transcription factor was recently shown to regulate expression of another G-protein-coupled receptor (Senga et al., 2003). To test this hypothesis, we first checked whether uPA could activate Stat3 in MCs. Indeed, stimulation with uPA caused a significant increase in Stat3 tyrosine phosphorylation, as shown in immunoblotting experiments using an antibody that specifically recognized Stat3 phosphorylation on Tyr 705 (Fig. 4A). Stat3 activation was time-dependent and reversible, peaking after 20 minutes of uPA stimulation. This activation was specific for Stat3, as no changes in phosphorylation state of other Stat proteins, namely Stat1, Stat2, Stat4 and Stat5 were observed (data not shown). To determine whether uPA-induced activation of Stat3 results in its translocation to the cell nucleus as required for the functional effect

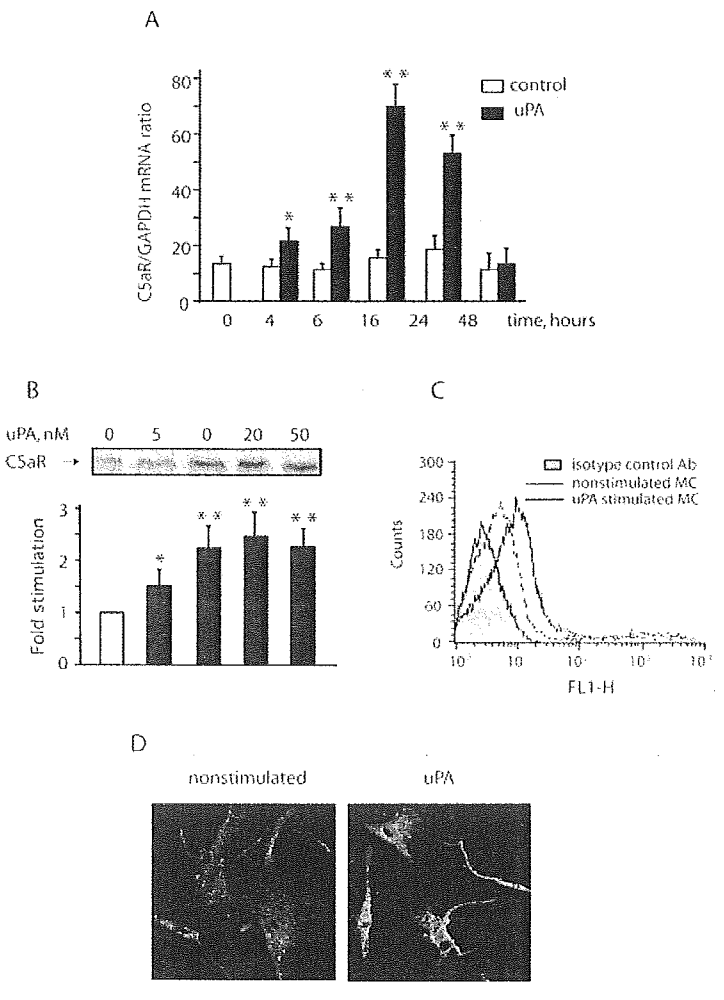

Fig. 1. uPA upregulates expression of C5aR in MCs. (A) RT-PCR analysis for C5aR mRNA was performed using the TaqMan method. RNA was isolated from quiescent MCs incubated for the indicated times with 20 nM uPA or in medium without uPA (control). *GAPDH* served as a house keeping gene. The results are presented as mean ± s.e.m. of four separate and independent experiments. (B) The quiescent MCs were stimulated for 20 hours at 37°C with the indicated concentrations of uPA, and C5aR protein was visualized in the membrane fractions by immunoblotting with anti-C5aR antibodies. MCs incubated in medium without uPA served as a control. The data on the upper panel are representative of four separate and independent experiments. Quantification of the results of these experiments by densitometry presented as mean ± s.e.m. is shown in the lower panel. Significance between control unstimulated and stimulated cells was determined by Student's *t*-test (*P<0.05; **P<0.01). (C) FACS analysis of MCs stimulated (solid line) or not (dashed line) for 20 hours at 37°C with 20 nM uPA using a FITS-labeled murine monoclonal anti-C5aR antibody. FITS-labeled isotype-matched antibody was used as a negative control (grey area). The results are representative of two separate and independent experiments. (D) The quiescent MCs were stimulated for 20 hours with 20 nM uPA or in medium without uPA (control). The cells were then fixed and stained with primary anti-C5aR antibodies and Alexa Fluor 488-conjugated secondary antibodies. Results are representative of three separate experiments.

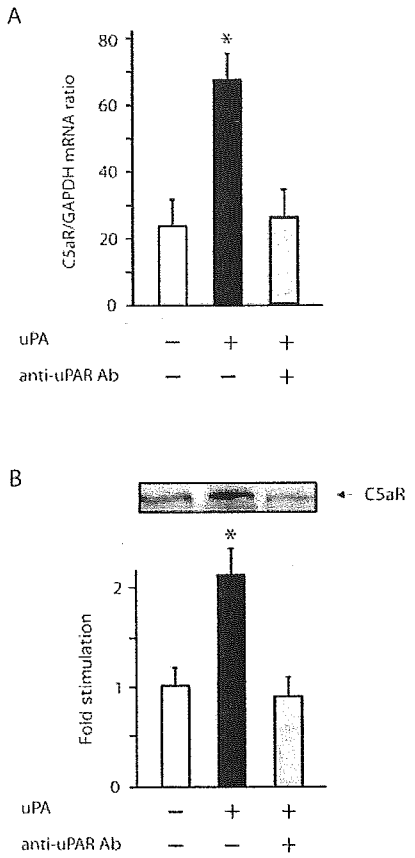

Fig. 2. uPAR mediates uPA-dependent upregulation of C5aR expression. The quiescent MCs were stimulated for 20 hours with 20 nM uPA in the presence or absence of 5 μg/ml anti-uPAR monoclonal antibody, and C5aR expression was investigated at the mRNA (A) and protein (B) levels using RT-PCR TaqMan analysis and western blotting, respectively. MCs incubated in medium without uPA and anti-uPAR antibody served as a control. The results in A are presented as mean ± s.e.m. for three separate and independent experiments. The data on the upper panel in B are representative of three separate and independent experiments. Quantification of the results of these experiments by densitometry presented as mean ± s.e.m. is shown in the lower panel. Significance between control unstimulated and stimulated cells was determined by Student's *t*-test (*P<0.05).

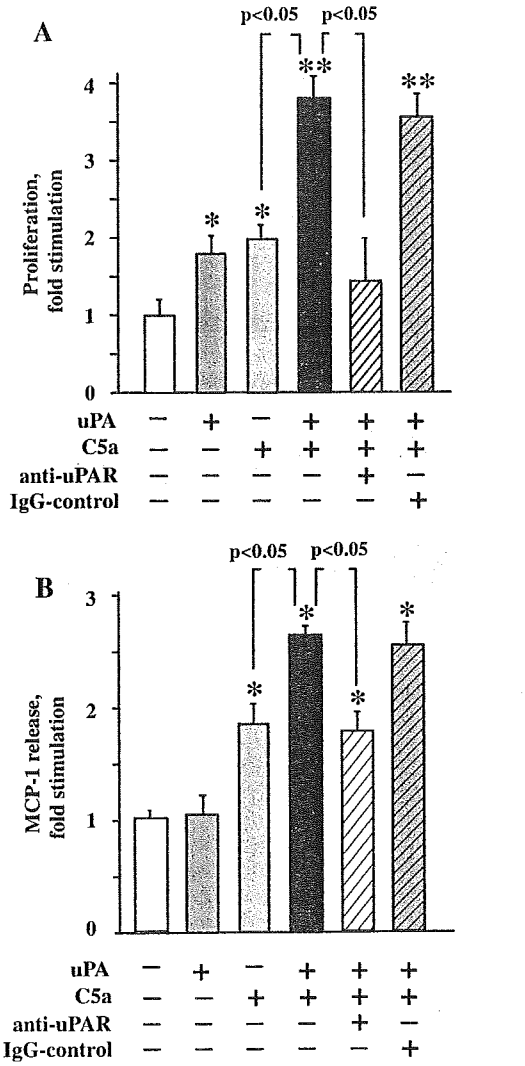

Fig. 3. uPA potentiates C5aR-related responses in MCs. (A) Quiescent MCs were incubated in 96-well microtiter plates with 20 nM uPA or 20 nM C5a alone or in combination with both stimuli in the presence or absence of 5 μg/ml anti-uPAR monoclonal antibody or irrelevant mouse IgG for 24 hours. The cells incubated in medium without stimuli served as a control. After 16 hours labeling with BrdU DNA synthesis was used as measure of the proliferation rate. Results are given as mean ± s.e.m. of four independent experiments performed in six parallel wells for each condition. (B) MCP-1 release was evaluated in supernatants from MC monolayers that were incubated as described in A for 48 hours. MCs incubated in medium without stimuli and producing 868±95 pg/ml MCP-1 served as a control. The data are given as mean ± s.e.m. of four separate and independent experiment performed in triplicate for each condition. Significance between control unstimulated and stimulated cells, as well as between the cells stimulated in the presence or not of 5 μg/ml anti-uPAR monoclonal antibody was determined by Student's *t*-test (*P<0.05; **P<0.01).

of Stats on gene transcription, immunocytochemical studies were performed. As shown in Fig. 4B, Stat3 translocated efficiently into the nuclei of MCs stimulated with uPA.

Phosphorylation of signal transducers and activators of transcription of the Stat family is mediated via the Janus kinases (Jaks) (Chatterjee-Kishore et al., 2000; Darnell et al., 1994). This interplay is highly specific, thus contributing to the specificity of cell functional responses to cytokines, growth factors and polypeptide hormones utilizing the Jak/Stat pathway for signal generation. We therefore examined activation of Jaks in MCs stimulated with uPA. Treatment with uPA rapidly increased specific tyrosine phosphorylation of the Janus kinase Tyk2 (Fig. 5A), whereas other Jaks, namely Jak1, Jak2 and Jak3 were not affected (data not shown). The kinetics of this activation correlates with those for Stat3 phosphorylation. To provide more direct evidence that the uPA-induced Stat3 phosphorylation was really mediated by Tyk2, a dominant negative form of Tyk2, devoid of kinase activity, was